

StrainWise

Deliverable D1.2

Final report

Grant Agreement Number	: 270658
Project Title	: Hardware & Software Development of Wireless Sensor Network Nodes for Measurement of Strain in Airborne Environment
Deliverable Type	: Periodic report

Deliverable Number	: D1.2
Title of Deliverable	: Final report
Nature of Deliverable	: Report
Contractual Delivery Date	: February 28, 2013 – T0 + 28
Actual Delivery Date	: February 28, 2013
Contributing WPs	: WP1, WP2, WP3, WP4, WP5, WP6, WP7
Author(s)	: Damien Piguet (CSEM), Jean-Dominique Decotignie (CSEM), Georges Bailleul (Serma), Christophe Leroux (Serma), Michalis Kiziroglou (Imperial College), Eric Yeatman (Imperial College)

Abstract

This document is the official final report on the Cleansky JUT project *Strainwise*, as required by the European Commission. It corresponds also to deliverable D1.2 "Final report" of the project's list of deliverables.

The Strainwise project aims at demonstrating a wireless and energy-autonomous sensing system dedicated to the measurement of strain in commercial aircrafts.

The project started on the 1st of November, 2010 and finished on December 31st, 2012.

The report follows the template published by the European Commissions. The topics covered are: executive summary, context and objectives, main S & T results / foregrounds and potential impact.

Keyword list

Wireless Sensor Network, Aircraft, Low Power, Strain Sensor, Energy harvesting

Table of contents

1	Executive summary	6
2	Context and main objectives	7
2.1	<i>Project global objectives</i>	7
2.2	<i>Consortium</i>	9
2.3	<i>Project structure</i>	9
3	Main S & T results / foregrounds	10
3.1	<i>Architecture</i>	10
3.1.1	Network architecture	10
3.1.2	Sensor node	10
3.1.3	Wireless data concentrator	11
3.1.4	Firmware architecture and development method	12
3.1.5	WSN server	13
3.2	<i>Wireless communication</i>	13
3.2.1	Protocol	13
3.2.2	Synchronisation	14
3.2.3	Evaluation	16
3.3	<i>Power supply</i>	22
3.3.1	Device Concept	22
3.3.2	Device Fabrication	23
3.3.3	Power Electronics Interface	24
3.3.4	Power Supply Performance	24
3.4	<i>Packaging</i>	25
3.5	<i>Functional and qualification tests</i>	28
3.5.1	Functional tests	29
3.5.2	Flight clearance	31
4	Potential impact, dissemination and exploitation	33
4.1	<i>Impact</i>	33
4.2	<i>Dissemination</i>	33
4.2.1	Scientific papers	33
4.2.2	Within Cleansky SFWA ITD	34
4.2.3	Within the topic manager Airbus and EADS	34
4.2.4	To the general public	34
4.3	<i>Exploitation</i>	35
4.3.1	Sensor nodes purchased by Airbus FTI	35
4.3.2	New Cleansky project: Flite-Wise	35
4.3.3	Industrial partner Serma	35
4.3.4	Imperial college	35
4.3.5	CSEM	37
5	Project public website	38

List of figure

Figure 1: StrainWise network architecture as envisioned by Airbus	7
Figure 2: VTP measurements position (drawing provided by Airbus)	8
Figure 3: load pin (drawing provided by Airbus).....	8
Figure 4: network architecture	10
Figure 5: Sensor node architecture	11
Figure 6: Wireless data concentrator architecture.....	12
<i>Figure 7: C/C++ wrapper for embedded code simulation</i>	<i>12</i>
<i>Figure 8: architecture of the embedded protocol implementation</i>	<i>12</i>
<i>Figure 9: WSN server screenshot</i>	<i>13</i>
Figure 10: wireless synchronisation for time-stamping	15
Figure 11: wired synchronisation protocol.....	16
Figure 12: average time-stamping error vs. quartz tolerance	17
Figure 13: test setup with embedded devices. One cell.....	18
Figure 14: test setup with embedded devices. Two cells.....	18
Figure 15: extract of the same triangle signal acquisition by two sensor nodes in one cell.....	19
Figure 16: the synchronisation error is computed from the time difference between the two peaks of the acquisitions of the same triangle signal by sensor nodes 1 and 2.....	19
Figure 17: computation of peak time from data samples through interpolation and intersection.....	20
Figure 18: synchronisation error within one cell of two sensor nodes. Each point represents the synchronisation error computed on one cycle of the triangle waveform acquired by the sensor nodes.....	20
Figure 19: synchronisation error within two cells of one sensor node each. Each point represents the synchronisation error computed on one cycle of the triangle waveform acquired by the sensor nodes.....	21
<i>Figure 20: Schematic of the heat storage thermoelectric energy harvester.</i>	<i>22</i>
<i>Figure 21: (a) Direct thermoelectric harvesting. Heat availability is practically unlimited and optimum operation requires thermal resistance matching. (b) Heat storage thermoelectric harvesting architecture. Maximum thermal resistance is required.</i>	<i>23</i>
Figure 22: Photograph of device prototype.	23
<i>Figure 23: Block diagram of the power management electronics.</i>	<i>24</i>
Figure 24: Performance of the StrainWiSe power supply: (a) HSU temperature and TEG voltage; (b) TEG and rectifier power output and power delivery to the battery; (c) Cumulative energy at the TEG output, rectifier output and battery input; (d) Power supply output voltage characterisation showing battery voltage, regulator voltage and output power on a 100 Ω load.....	25
Figure 25: external aspect of the sensor node packaging	25
Figure 26: inside of the sensor node packaging. The power control PCB (Imperial College) is on the left of the heat storage unit and the data acquisition and communication PCB (CSEM) is on the top.....	26
Figure 27: connector between the two electronic boards.....	26
Figure 28: spring contacts used for connecting the energy harvester to the power PCB.....	26
<i>Figure 29: battery pack as an alternative power supply for the sensor node.....</i>	<i>27</i>
Figure 30: Integrated Sensor Node	27
Figure 31: Integrated WDC.....	28
Figure 32: Specific power supply electronic board for WDC.....	28
<i>Figure 33: Battery pack</i>	<i>28</i>
Figure 34: Strain Gauge simulator (PXI Card)	29
Figure 35: test setup with battery powered sensor nodes.....	29
Figure 36: test setup with harvester-powered sensor node and strain gauge simulator	30
Figure 37: Sensor Node on vibration shaker on Z axis	32
Figure 38: Two Sensor Nodes in radiated emission test.....	32

List of tables

Table 1: summary of verification tests results	31
Table 2: flight clearance qualification requirements for the StrainWise system.....	31

1 Executive summary

(Please provide an executive summary. The length of this part cannot exceed 1 page.)

The StrainWise project realised a wireless and energy autonomous strain monitoring system for commercial aircraft. It is the result of the integration of state-of-the-art low power electronics with innovative solutions in the fields of ultra-low power wireless communications and thermo-electric energy harvesting.

The system aims at providing the aircraft operators with a new tool for the predictive maintenance of airframes, with minimal weight impact and low usage costs. The main benefit of such tools is a significant reduction of maintenance costs by replacing regular checks that imply the automatic substitution of elements that have gone through their quota of flight cycles or hours by the analysis of the load endured by the aircraft structure during the flights. Then, maintenance actions can be decided for the aircraft parts that are indicated as potentially weakened or damaged by the analysis. The minimal weight impact stems from reduced cabling due to the wireless nature of the system. The usage and maintenance costs of the load monitoring system are low thanks to the combination of energy scavenging and ultra-low power communications as this eliminates the need for batteries and their regular replacement and assures a long system life.

The project targeted two specific use cases. The first use case addresses load monitoring in widely distributed pilot points of the Vertical Tail Plane (VTP) of commercially exploited aircraft. Measurements sessions are triggered by the Aircraft avionics when a flight sequence that may involve heavy loads on the VTP is detected from the observation of other flight parameters. One expects up to 10 measurements sessions of 30 s per flight. The second use case describes the monitoring of strain in the landing gear. In this case, measurements are acquired continuously during the landing phase from landing gear extension until the aircraft has reached a low speed on the ground. The specified maximal data acquisition duration is 500 s.

For both use cases, specified measurements sampling frequencies are between 120 and 500 Hz. All data samples have to be stamped with the aircraft time with a synchronisation error of at most 1 ms.

A specific Time-Division Multiple Access (TDMA) protocol has been developed to fulfil the requirements for the data acquisition chain. It automatically adapts its duty cycle to the traffic needs in order to minimise energy consumption, so that the autonomous power supply is sufficient. During flight, the maximal wake-up delay is 0.5 s. The protocol is reliable because it supports repetitions. Moreover, it integrates a synchronisation mechanism that is very light in terms of protocol overhead. Experiments made with the current implementation have shown 100% packet arrival success rate and a maximal synchronisation error of less than 600 μ s on the data timestamps within a single cell. If several cells are used the synchronisation error is still below 1 ms using a simple synchronisation algorithm for the network wired part.

A power supply based on thermoelectric energy harvesting that utilises a heat storage unit (HSU) partially filled with a phase change material (PCM) was designed and tested. This method, initially proposed by EADS, was previously described in deliverables D1.1 and D5.1. Various types of PCMs were tested based on the flight temperature profile provided by Airbus. The temperature gradient was converted into usable electrical power using thermoelectric generators (TEGs). In a flight cycle, phase change occurs twice which causes the generated voltage from the TEGs to switch polarity. The TEGs were observed to generate approximately 1 V peak voltage for a temperature gradient of 20°C. Rectification of the TEG voltage was performed using a new and custom-designed rectifier topology. The power management electronics developed for this application enabled the harvested energy to be used to recharge an internal battery and also to supply electrical power to transmit strain gauge data wirelessly.

The system built within the StrainWISE project comprises the following entities: an energy autonomous Sensor Nodes (SN), a Wireless Data Concentrators (WDC) and a Wireless Sensor Network server (WSN server). All entities have been fully implemented in hardware/software and successfully went through functional and qualification tests. Specifically, the qualification tests showed that the devices can sustain heavy vibrations (DO-160¹ Cat. R Curve C1) and extreme temperatures (+85 to -55 °C) whilst respecting a challenging maximal electro-magnetic field emissions constraint (DO-160 Cat. H Curve C1). A complete StrainWise system has been delivered to Airbus for in-flight tests.

¹ "Environmental Conditions and Test Procedures for Airborne Equipment", EUROCAE ED14 / R.T.C.A. DO-160

2 Context and main objectives

(Please provide a summary description of the project context and the main objectives. The length of this part cannot exceed 4 pages.)

2.1 Project global objectives

The goal of the StrainWISE project is to demonstrate the benefits of Wireless Sensor Networks (WSN, smart sensors with a radio interface) applied to the monitoring of aircraft elements such as engines, structures, landing gear, etc. Advantages over today's wired solutions are reduced wiring costs and weight as cabling is eliminated and flexibility to be deployed on-board aircraft without requiring a redesign of the data wiring layout.

To this end, the StrainWISE project aims at developing an advanced wireless sensor platform to which strain gauges can be connected. It is able to operate on the wings of the aircraft without maintenance for the plane lifetime, thanks to embedded energy harvesters and ultra-low-power design. The idea is to build an integrated autonomous platform which is specifically optimized to fill the requirements drafted by Airbus, the main commercial aircraft manufacturer of Europe.

The support of the following functions is targeted:

- Sensor acquisition and logging
- Wireless network configuration and start
- Management of operational modes
- Local production of energy (scavenging)
- Local management of energy
- Remote acquisition of data and its configuration.

On top of the functional requirements, the project addresses flight clearance qualification for harsh environmental conditions (vibrations, high temperature range) and radiated emissions.

The project is responsible to realise and integrate all the entities to be part of the platform (see Figure 1):

- A wireless Sensor Node (SN) with an energy harvester
- A Wireless Data Concentrator (WDC) responsible to manage several SN and to forward their data to a server over a wired link.
- A Wireless Sensor Network server (WSN server) responsible to collect, store and display measurements data and to provide a human interface for the system configuration and management.

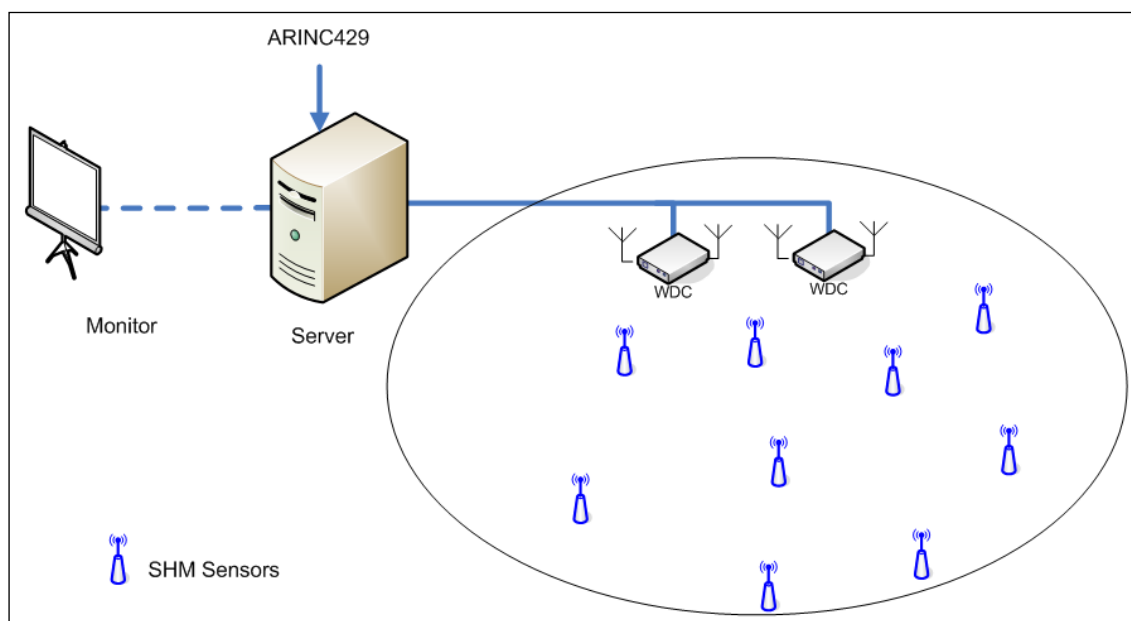


Figure 1: StrainWise network architecture as envisioned by Airbus

The system is dimensioned according to two use cases written by the topic Manager Airbus.

The first use case is the overload assessment in the Vertical Tail Plane (VTP). It involves the installation of 8 to 12 sensors in pilot points such as those depicted in Figure 2.

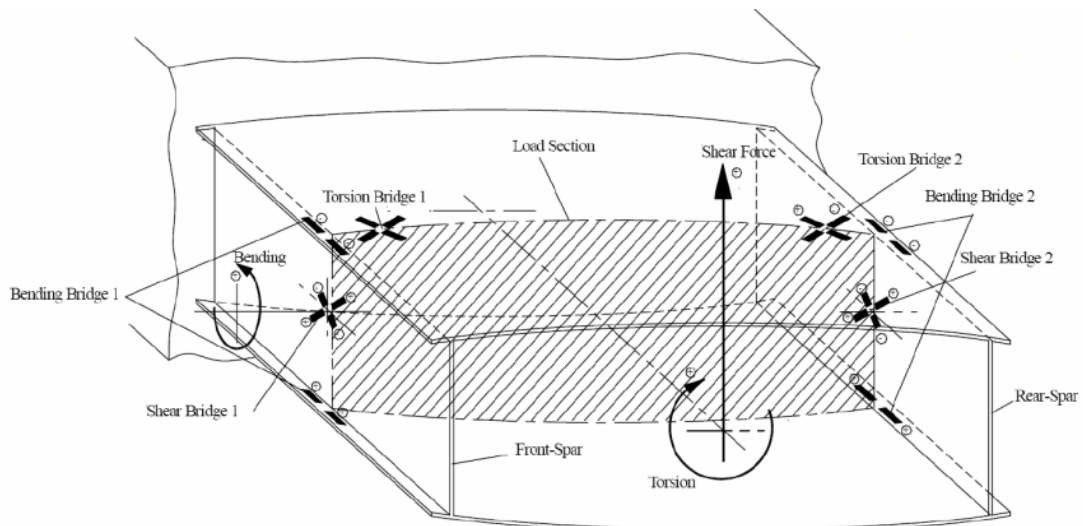


Figure 2: VTP measurements position (drawing provided by Airbus)

The measurements acquisition sequences defined by the use case are a 300 seconds long calibration during take-off and up to 10 on-demand sessions that can last for up to 30 seconds.

The second use case addresses the overload assessment in the landing gear for hard landing detection. It intends to replace an existing inert load-bearing pivot pin with a load measurement pin with embedded strain gauges (Figure 3).

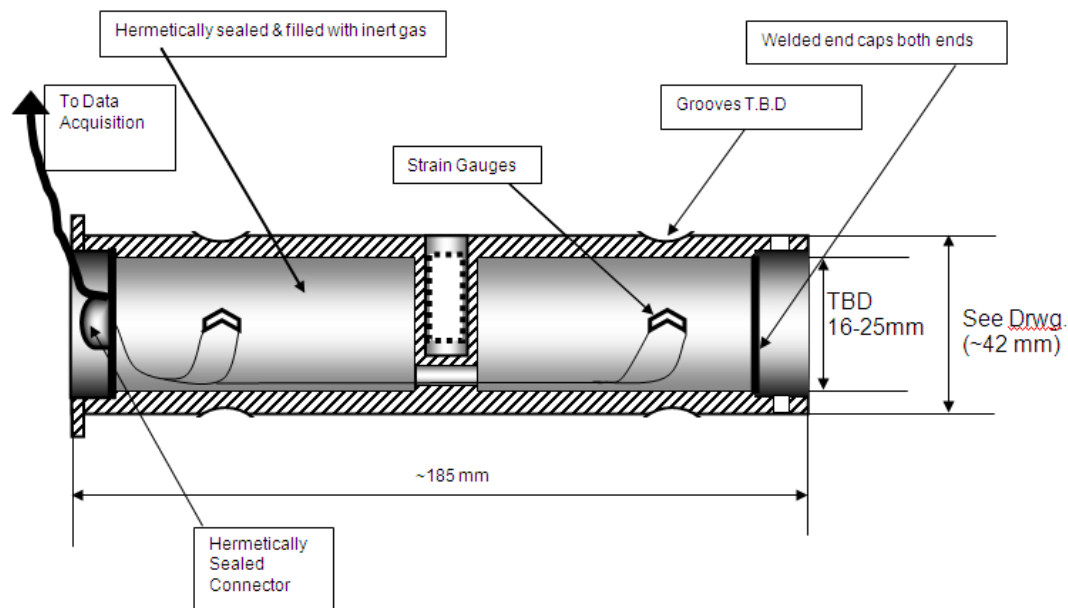


Figure 3: load pin (drawing provided by Airbus)

Like in the first use case, a calibration session of 300 seconds is specified. It is to be followed by a unique 500 seconds long measurement session during the landing phase of the aircraft.

Other important requirements that are common to both use cases are a sampling rate of 120 to 480 Hz; 12 bits sensor resolution and measurements samples time-stamping with a maximal error of 1 ms with respect to the aircraft global time. The system could comprise up to 200 sensor nodes in a single aircraft, while a cell (group of sensor nodes attached to the same wireless data concentrator) may contain up to 20 sensor nodes.

Finally, the project objectives comprised two test campaigns. The first campaign addressed laboratory functional and qualification tests to assess the system versus the requirements and to obtain flight clearance. The second test phase goal was to prove the system in flight, though not necessarily in a location specified by the use case.

2.2 Consortium

The consortium is made of three highly qualified complementary entities. The members are CSEM Centre Suisse d'Électronique et de Microtechnique (CH), Imperial College London (GB) and Serma Ingénierie (FR). CSEM brings its expertise in WSN and ultra-low power electronics. SERMA, an experienced actor in the aeronautics technology, brings expertise in the aeronautics environment and constraints, as well as production and test facilities. Imperial College London, one of the world leading laboratories, provides the scavenging and energy management expertise.

2.3 Project structure

To meet its ambitious objectives, the project is divided into one management work package and six technical work packages, where each of them addresses a particular aspect of the work.

Work Package 2 "Platform Architecture" studies the architecture of the strain sensing platform and defines the interfaces between the subsystems composing it to steer the development of the network architecture (WP3), sensor front-end (WP4) and power supply (WP5). Additionally, WP2 is responsible for the specification of test plans at high-level. Work package 3 "Network Architecture" defines and implements the different protocols necessary for the autonomous platform. A multi-star architecture (multiple sinks interconnected by a backbone) with a deterministic channel access is the preferred approach to meet safety and latency requirements. Robustness can be further increased using redundant connectivity and antenna diversity. The main challenge is still the power efficiency due to long lifetime and limited energy supply.

The goal of the fourth work package "Sensor Front-End" is to define and implement an ultra-low power sensor front-end for strain gauge read out including data pre-processing with capabilities for temperature and gauge factor compensation.

Work package 5 "Power Supply" deals with the design and development of a miniature energy harvester for in-aircraft power supply of the wireless sensors as battery solutions are not acceptable, for reasons of reliability, safety and maintenance (recharging or replacement) costs. Energy harvesting devices collect locally available ambient energy and transform it into electrical. At the intended sensor node locations, two types of energy are available: vibration and the heat energy that corresponds to the temperature variations of the aircraft during flights. An early assessment of availability indicated that a thermoelectric harvesting system may be preferable. Therefore, a thermoelectric harvesting power supply is being developed. The objective is to meet the energy availability, demand and size specifications required for the sensor nodes. Whatever the energy source, the energy harvester and the power processing electronics should be co-designed to maximise efficiency and dependability in the smallest possible package.

The last two work packages deal with testing and system validation. WP6 "Demonstrator Build-Up and Lab Tests" focuses on the laboratory tests that will evaluate the features provided by the development work packages. It also performs flight clearance qualification tests to be authorised to install the system inside an aircraft for the in-flight tests that will be performed in WP7 "Ground and Flight Tests". The objective of WP7 is to assess the system's actual performance and to evaluate the individual features of the designed modules in real flight conditions.

3 Main S & T results / foregrounds

(Please provide a description of the main S & T results/foregrounds. The length of this part cannot exceed 25 pages.)

This section describes the main scientific and technological results delivered by the StrainWise project. The main contributions pertain to the wireless communications and synchronisation, low-power electronics and energy scavenging domains. Moreover, the project realised the packaging and the qualification tests of the system.

Before detailed the technical contributions, the system architecture is briefly described in the next subsection.

3.1 Architecture

The StrainWise system architecture was built from the analysis of the requirements published by the topic manager Airbus.

3.1.1 Network architecture

The StrainWISE network architecture is that of a multi-cell Wireless Sensor Network (WSN). Wireless cells are linked to a central server (the avionics) through a wired network (Ethernet). Each cell consists of a Wireless Data Concentrator (WDC) and one to 20 Sensor Nodes (SN). The responsibilities of the WDC are the configuration of the cell (sensor nodes discovery), the control of the TDMA (SN transmission slot assignation), the relaying of commands and data between the server and the SNs and the synchronisation of the cell with the server time. The WDC is connected to the aircraft power supply, thus it does not have any energy constraint. In contrast, a sensor node has to provide its own energy. Its task is to perform the strain measurements on request from the server and to transmit them via its assigned WDC. Figure 4 details the network architecture.

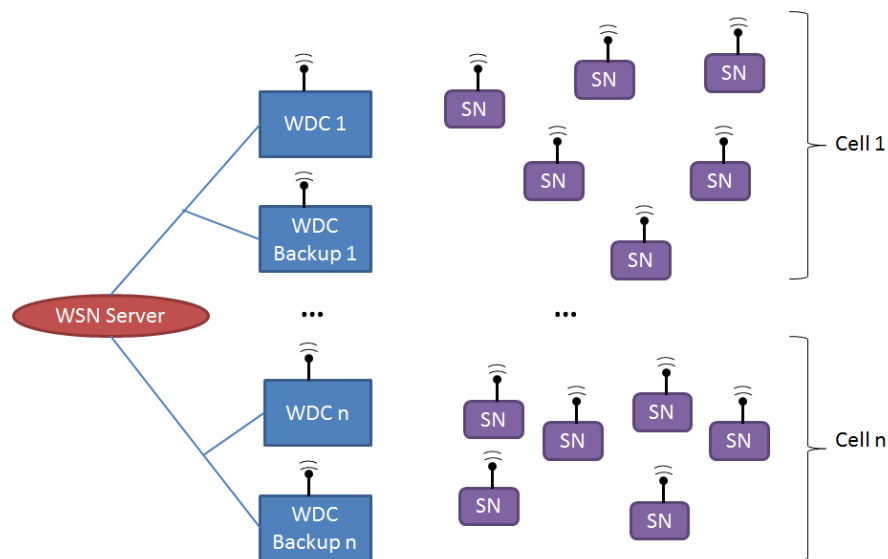


Figure 4: network architecture

As shown in Figure 4, a cell may have an optional extra WDC (the Backup WDC), which is used to improve the cell robustness, as will be explained in section 3.2.

The following paragraphs detail the architecture of the SN, WDC and WSN server.

To reduce development costs, the SN and WDC platforms have many common parts. The first difference between them is that the SN has an analogue to digital (ADC) circuit to acquire measurements and that the WDC has a wired interface to the WSN server (Ethernet port). Secondly, the sensor node is powered by its energy harvester whilst the wireless data concentrator is powered by the aircraft power supply network.

3.1.2 Sensor node

The sensor node block diagram is shown in Figure 5. The system wireless communication interface is an Atmel AT86RF231/233. It supports antenna diversity for better reliability. The

system is controlled by a Texas Instrument MSP430F5437A MCU. Among its advantages are numerous serial interfaces (UART/SPI/I²C), large RAM and program memory space, as well as low power consumption in operation and an ultra-low power sleep mode. The MCU controls the measurement acquisition performed by a Semtech SX8724S ADC, which is connected to the strain sensor (a Wheatstone bridge strain gauge). This particular chip has been chosen because of its low current consumption, especially in sleep mode. A 1 MB low power flash memory has been added to allow the recording of all measurements performed during a typical flight as described in the use cases (section 2.1) if the wireless communication fails.

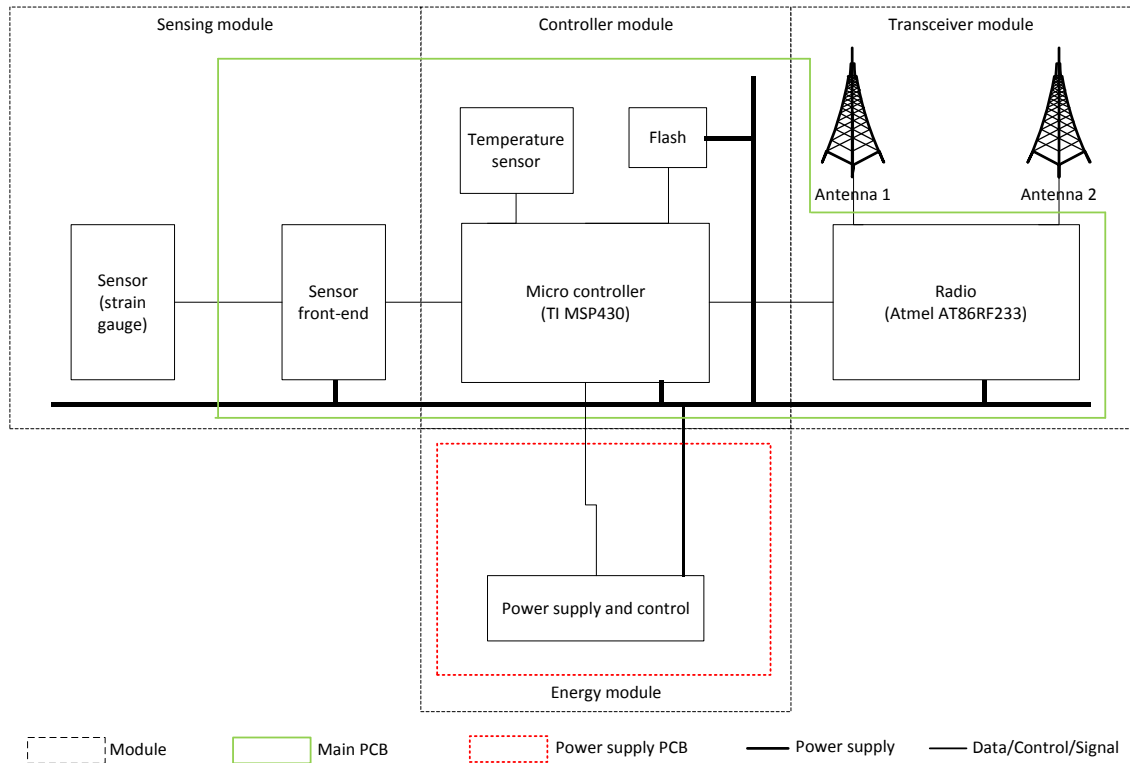


Figure 5: Sensor node architecture

Sensing, controller and transceiver parts are on the same PCB whilst the power supply electronics are put on a second board. This distribution is optimal in terms of size, flexibility and project management (development by separate teams).

3.1.3 Wireless data concentrator

The wireless data concentrator (Figure 6) shares the controller and transceiver modules with the sensor node. However, it does not have an ADC because it does not acquire measurements. Also, its power supply is simpler because the device is powered by the aircraft network. Finally, the WDC has an Ethernet port for the communication with the WSN server. Size and environment constraints led to the choice of a Lantronix XPort².

² <http://www.lantronix.com/>

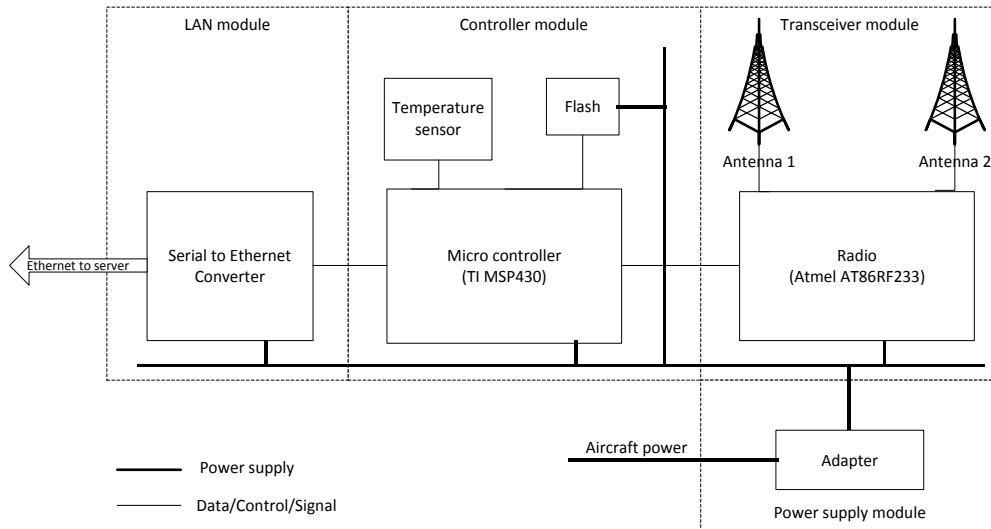


Figure 6: Wireless data concentrator architecture

3.1.4 Firmware architecture and development method

The original aspect of the firmware implementation strategy is that the communication protocol and data acquisition codes are written for the embedded platform from the start, but that the development work is done within a simulator to speed-up the development, to ease the debugging and evaluation. A wrapper has been written in the simulator to translate calls to the embedded OS functions to the simulator counterparts (Figure 7).

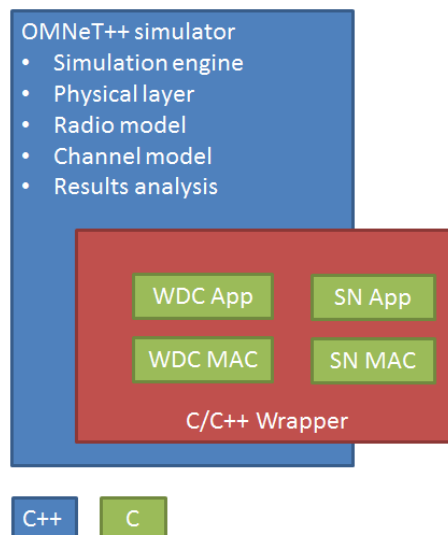


Figure 7: C/C++ wrapper for embedded code simulation

Once validated in the simulator, the protocol implementation is then simply moved to the embedded platform as depicted in Figure 8. In this configuration, the protocol code interfaces with the drivers without any further modification thanks to the early development in the simulator wrapper.

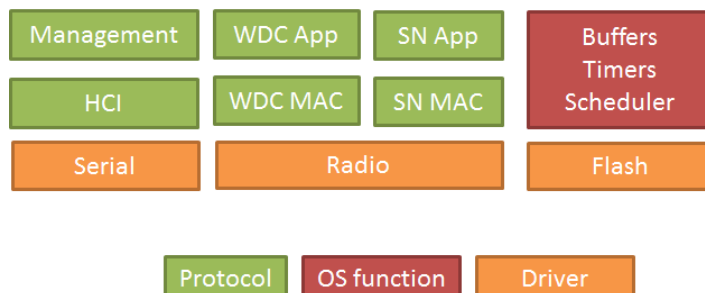


Figure 8: architecture of the embedded protocol implementation

3.1.5 WSN server

The server was developed as a LabView[®]³ application. The reasons for choosing this environment are flexibility (the server can be installed on any computer), ease of use (the tool is commonly used by non-IT people in laboratories) and the ability to be modified and connected to other systems. The server is available as a stand-alone executable that can run on computers which do not have a LabView license. The sources are also provided so that a user equipped with the full development version of LabView can modify it.

The WSN server can configure and control up to three cells. Although the network supports more, the three cells limitation limits the server complexity. Several server instances can run in parallel to allow the control of several networks.

The server relies on the TCP/IP module of LabView to communicate with one or several WDCs. LabView relies in turn on the underlying OS. A screen shot is shown in Figure 9.

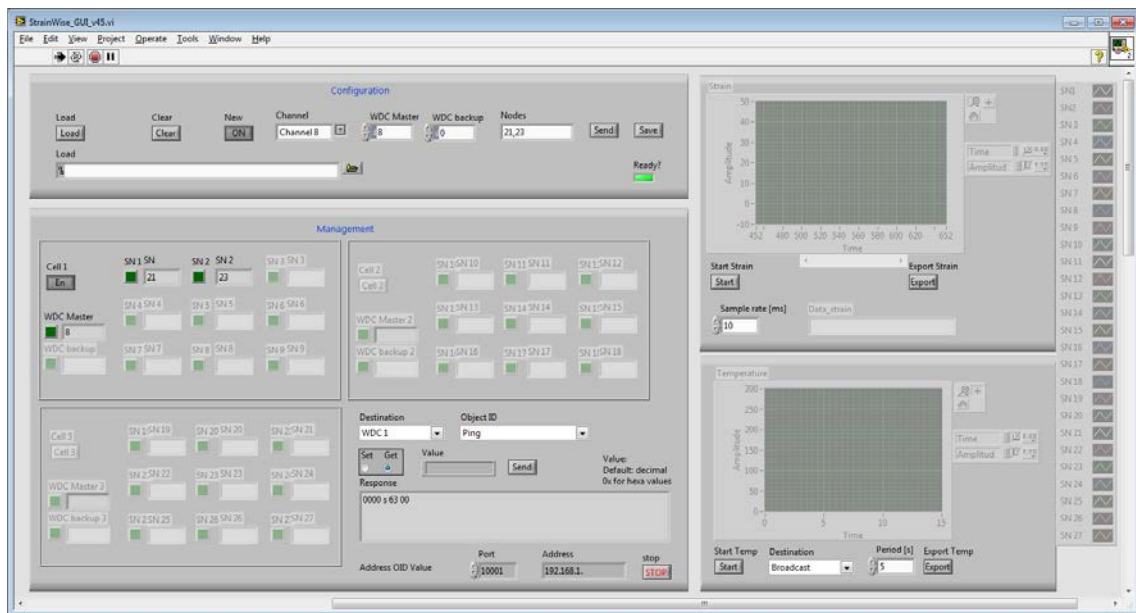


Figure 9: WSN server screenshot

3.2 Wireless communication

The system wireless communication part faces numerous challenges. First, it has to support up to 1 kB/s useful data rate per node (2 bytes samples at 500 Hz acquisition rate) during the acquisition and up to 20 nodes per cell (as specified). Second, the nodes must be synchronised with the server to allow the time-stamping of each data sample. Third, power consumption must be minimal to ensure that the sensor node does not consume more than its associated energy harvester generates. Especially, long aircraft parking phases are critical because one cannot expect the energy harvester to generate power when the aircraft is not in use. Finally, the wireless communication protocol must support a system installation procedure that minimises human intervention.

3.2.1 Protocol

The proposed protocol is of TDMA type to cope with airworthiness regulations which impose deterministic protocols. Also, it is single hop since none of the foreseen use cases imposes multi-hop requirements, according to connectivity measurements performed by partner CSEM on aircrafts. To keep sensor node energy consumption to a minimum, the main idea is to adapt the duty cycling to the operation phase whilst benefiting from the fact that the WDC is powered. The WDC is selected to be the master of the TDMA cell because it is powered and has a wired connection to the WSN server meaning that it can be synchronised with it.

Four modes of operation that relate to the different phase of operations have been identified after a careful use case analysis:

³ <http://www.ni.com/labview>

- **Configuration:** sensor nodes are on, but not yet associated to a WDC (e.g. before installation in a new aircraft). WDCs are either off or awaiting the association with all their assigned sensor nodes to complete.
- **Sleep:** during the flight, a cell is in a low power mode while not acquiring any measurements, but it can be awakened with a short delay.
- **Data transfer:** a cell is performing and transferring strain measurements.
- **Ultra-low power sleep:** SNs and WDCs are associated, but the aircraft is stored. The network sleeps deeply with a long wake-up delay.

In all four modes, the WDC broadcasts a beacon every 40 ms on a channel assigned by the WSN server. In **Configuration** mode, the list of addresses of the nodes pertaining to the cell is sent to the WDC from the server and broadcasted in the beacon. In this mode, each SN sleeps for 360 seconds, then wakes-up and listens to each channel for 40 ms. If a beacon that advertises the node address is received, the sensor node registers to the WDC, stays on the current channel and goes into **Sleep** mode. If no beacon is received after trying all channels, the node goes back to sleep for 360 seconds. A WDC switches to **Sleep** mode once every sensor node of its list has registered.

In **Sleep** mode, each sensor nodes synchronises on the *super frame* beacon which is a special beacon sent every k^{th} beacon by the WDC. The SN sleeps between two super frame beacons. In the current implementation, the super frame period is 12 beacons, meaning that the cell can be woken-up within 480 ms.

By changing a couple of bits in the beacon header, the WDC can switch its sensor nodes into **Data transfer** mode in which the SNs listen to every beacon. In this mode, the beacons contain a slot assignation section to allow the sensor nodes to transmit measurements or any command responses. The sensor nodes wake-up, either to listen to the next beacon, transmit a packet in their slot or acquire a measurement sample. The mode also supports an acknowledgement and repetition scheme to provide reliable data transmission. Acknowledgements are sent by setting the bits corresponding to the slots of a successful data reception to one in the following beacon. Sensor nodes repeat the last packet if an acknowledgement is not received. Measurements samples that are not yet sent are buffered in RAM, and, if necessary, in non-volatile memory.

When a sensor node loses connection with its assigned WDC, for instance when the latter one is turned off with the aircraft, the sensor node enters **Ultra-low power sleep** mode in which it listens for 40 ms on the assigned channel every 360 seconds and sleeps in between. It changes to **Sleep** mode as soon as a beacon from the assigned WDC is detected.

To increase the probability of successful beacon reception by sensor nodes, and, consequently, the rate of successful transmission, a backup WDC can be added to the cell. It will simply repeat the beacons sent by the master WDC.

3.2.2 Synchronisation

Synchronisation has been integrated to the communication protocol because measurement samples have to be stamped with the global system time. Because it is given by the WSN server, a synchronisation method was also implemented for the wired links between the WSN server and the WDCs.

3.2.2.1 Wireless

This paragraph describes the wireless synchronisation method integrated with the protocol. It is depicted in Figure 10. It assumes that the WDC is synchronised with the WSN server clock over Ethernet (green arrow on Figure 10), thus the WDC system time is equal to that of the server. It is also assumed that the TDMA MAC protocol operates in data transfer mode and that the sensor node acquires data. Data samples are kept in memory by the sensor node until they can be sent at the next transmission slot assigned by the WDC. Transmission slots are assigned in beacons regularly broadcasted by the WDC. Each beacon also contains a Beacon Sequence Number (BSN) that is incremented by the WDC at every beacon. Moreover, the WDC maintains a look-up table which associates each BSN with the time the corresponding beacon was transmitted. Hence the synchronisation protocol consists of the following steps:

1. The WDC sends a beacon with a sequence number and the slot allocation. The beacon transmission instant is saved in a look-up table.
2. Upon its slot time, the SN transmits the data samples which are in its buffer in a data packet. The data packet includes timestamps for the samples in the following form: the packet starts with the sequence number of the last beacon received from the WDC (the one which allocated the slot). The second field named 'offset' contains the amount of

time elapsed between the beacon reception and the acquisition of the first data sample transmitted in the packet. The third field is the acquisition period.

3. Upon reception of a data packet, the WDC replaces the beacon sequence number by the corresponding transmission timestamp recorded in the look-up table. Then the packet is forwarded to the WSN server.

Upon reception at the server, the timestamp of each sample can be computed. The timestamp of the first sample equals the beacon transmission timestamp plus the offset. Then the timestamp of the following samples are computed by adding the sampling period to the previous sample timestamp.

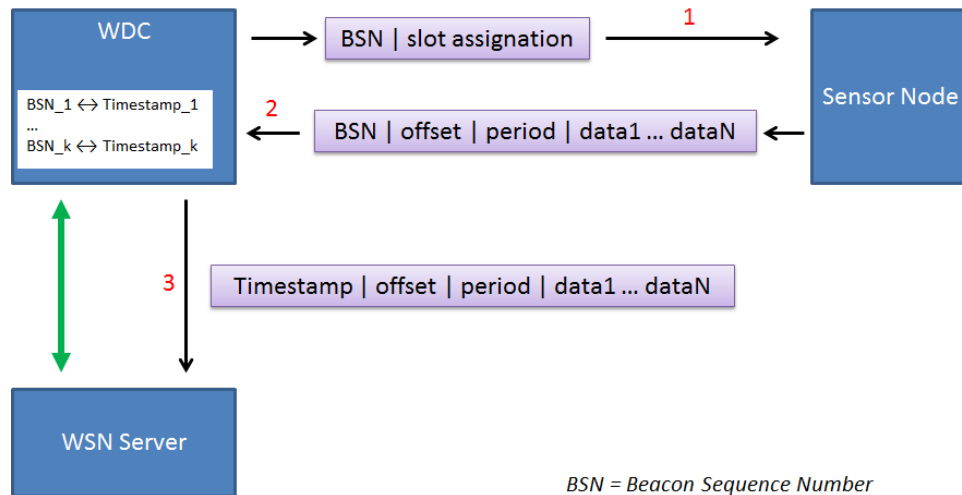


Figure 10: wireless synchronisation for time-stamping

3.2.2.2 Wired

The wired synchronisation protocol objective is to set the system time of all WDCs to the WSN server time. Practically, the protocol allows the WDC to compute its time difference with the server. This value is added to the beacon timestamps kept in the WDC look-up table mentioned in paragraph 3.2.2.1.

This value, named t_{diff} is always positive because the server, which is a Linux machine, has a system time originating in the years 1970's whilst the WDC system time starts from zero at boot time.

The synchronisation protocol used to compute the time difference estimate \hat{t}_{diff} uses the method introduced by Flaviu Cristian in 1989⁴. The message exchange depicted in Figure 11 provides the WDC with the four needed values t_1, t_2, t_3, t_4 : The WDC records t_1 and t_4 . t_2 and t_3 are provided by the WSN server in its responses to regular synchronisation requests sent by the WDC (period: 2 seconds).

⁴ F. Cristian, "Probabilistic clock synchronization", *Distributed computing*, 3:146-158, Springer-Verlag, 1989.

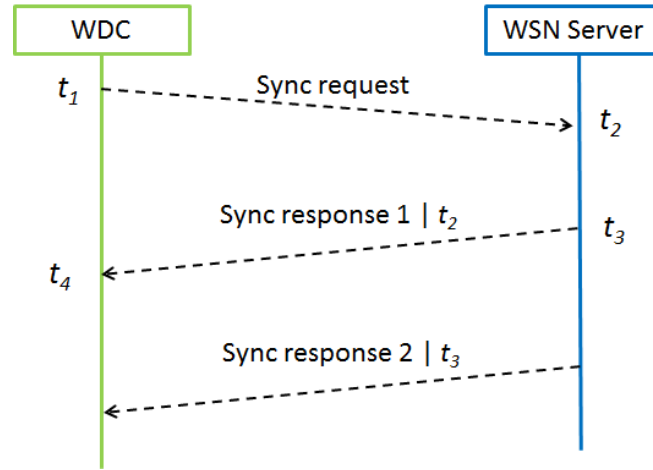


Figure 11: wired synchronisation protocol

The computation is done by the WDC. The estimate \hat{t}_{diff} is given by:

$$\hat{t}_{diff} = \frac{t_2 - t_1 + t_3 - t_4}{2}$$

This value is added by the WDC to the beacon transmission timestamps.

An implementation of a Linux synchronisation server using the above method has been delivered. It automatically selects the most accurate timestamps provided by the operating system installation (Linux supports network interface card timestamps, provided that required hardware and software driver are installed).

The next subsection presents the evaluation of the communication and synchronisation protocol.

3.2.3 Evaluation

At a maximal specified sampling rate of 500 Hz and two bytes per sample, each sensor node produces at most 1 kB of useful data per second. Setting the TDMA parameters to 1 ms for the slot duration, 40 ms for the beacon period and 20 nodes max per cell ensures that each sensor node receives enough bandwidth, given that the radio is used at its maximal bitrate of 1 Mb/s. Moreover, the protocol supports retransmissions and the nodes have enough RAM for buffering during short link disruptions. For this reason, packet arrival success rate simulations and tests are not interesting with respect to the protocol study, but only to verify the implementation correctness.

With respect to the application specification, time-stamping precision is essential to allow the comparison and matching of strain measurement data with other systems. Therefore, this evaluation concentrates on this aspect, first by means of simulations, then with measurements on the real implementation.

3.2.3.1 Simulations

The simulation scenario presented here shows the data transfer mode and the synchronisation principle used for time-stamping measurement data. The simulations have been performed with 1 ms slot duration and 40 ms beacon period, 20 SNs in the cell. It involves the triggering of a data transfer session, the transmission of all measurement samples to the WDC and the timestamp calculation for each received sample.

Measurement samples are created by each SN application: a 16-bit random value is picked each time a periodic timer expires.

The simulator used is OMNeT++. A C++/C wrapper has been written to develop and run the embedded protocol code in the simulator. A specific module fulfils the role of the WSN server: it computes the timestamps and saves each received value. The correctness of the computed timestamps is verified by comparing the timestamp reconstituted at reception with a timestamp recorded by the simulator at data generation for each sample.

The simulator allows the simulation of the quartz deviation. For each network entity, a quartz deviation value is randomly picked between $-T_q$ and $+T_q$, where T_q is the quartz tolerance, a

simulation parameter. The system times of the WDCs are not influenced by the quartz deviation because each WDC is assumed synchronised with the WSN server.

Additional simulation parameters are:

- Measurement rate: 100 Hz.
- Measurement session duration: 15 s
- Six values have been tried for the quartz tolerance: from zero to 100 parts per million (PPM), with steps of 20 PPM.
- For each quartz tolerance value, 50 simulation runs have been performed.

The mean absolute value difference between the timestamps at sample generation and the computed timestamps at reception versus the quartz tolerance is shown on the bar graph of Figure 12. The difference values have been averaged over all sensor nodes and all 50 runs for each quartz tolerance value.

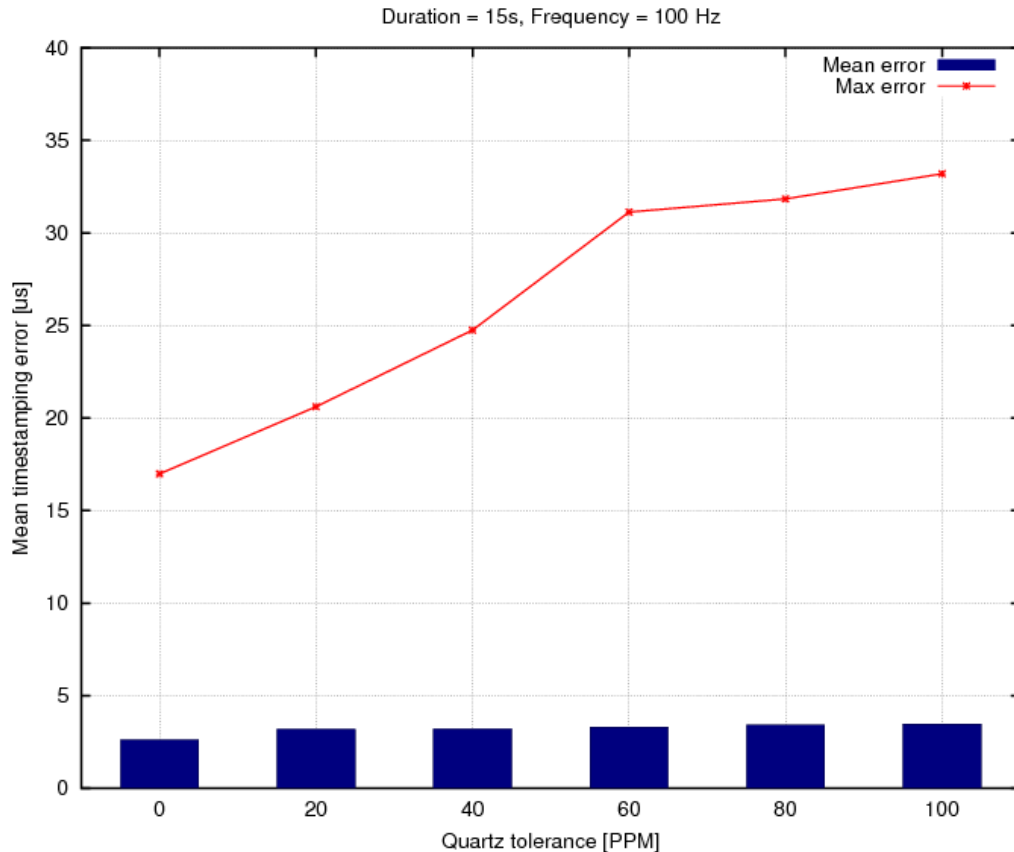


Figure 12: average time-stamping error vs. quartz tolerance

In the ideal case of a zero quartz deviation, an average error of about 2.5 μs is observed. This non-zero value is due to two factors: first, there is a difference in timestamp resolution: the timestamp at data generation is done by the simulator with a very high resolution, up to the nano-second, whilst the computed timestamp depends on the resolution to the micro-second of the code written for the embedded platform. The latter values are hence truncated to the micro-second. More important is the second factor: due to channel noise and attenuation, some beacons sent by the master WDC are missed by the sensor node. Instead, it receives that of the backup WDC. Of course, the timestamp computation compensates for the extra slot duration, but there is a radio switching delay of about 16 μs between the instant the backup WDC asks for the beacon to be sent and its actual transmission by the radio. Hence, a minority of the measurement timestamps suffer from a 16 μs error which negatively influences the average error depicted in Figure 12 above.

Also, Figure 12 shows an error worsening with the quartz tolerance as expected, but that still lies well below the 1 ms requirement. Therefore the whole data transfer and synchronisation chain as well as the current implementation are correct in the simulation.

The next subsection presents the results obtained with the real devices.

3.2.3.2 Embedded implementation

Transmission and synchronisation tests have been performed with two sensor nodes on two different setups. The first setup involves one cell with one WDC. In the second setup, each sensor node belongs to a different cell and the wired synchronisation protocol is active. To allow the measurement of the time-stamping difference, one signal generator has been used to input both sensor nodes via a double Wheatstone bridge circuit specifically developed to ensure that the two SNs measure the same signal on their differential input. The input signal is a triangle waveform. The setups are depicted in Figure 13 and in Figure 14.

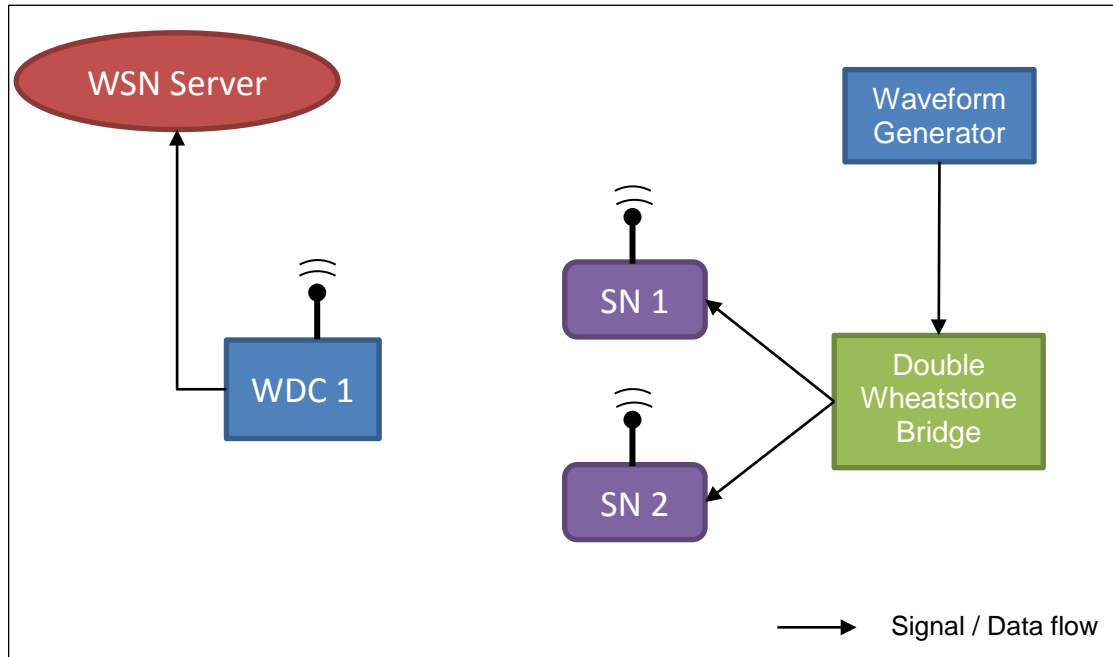


Figure 13: test setup with embedded devices. One cell.

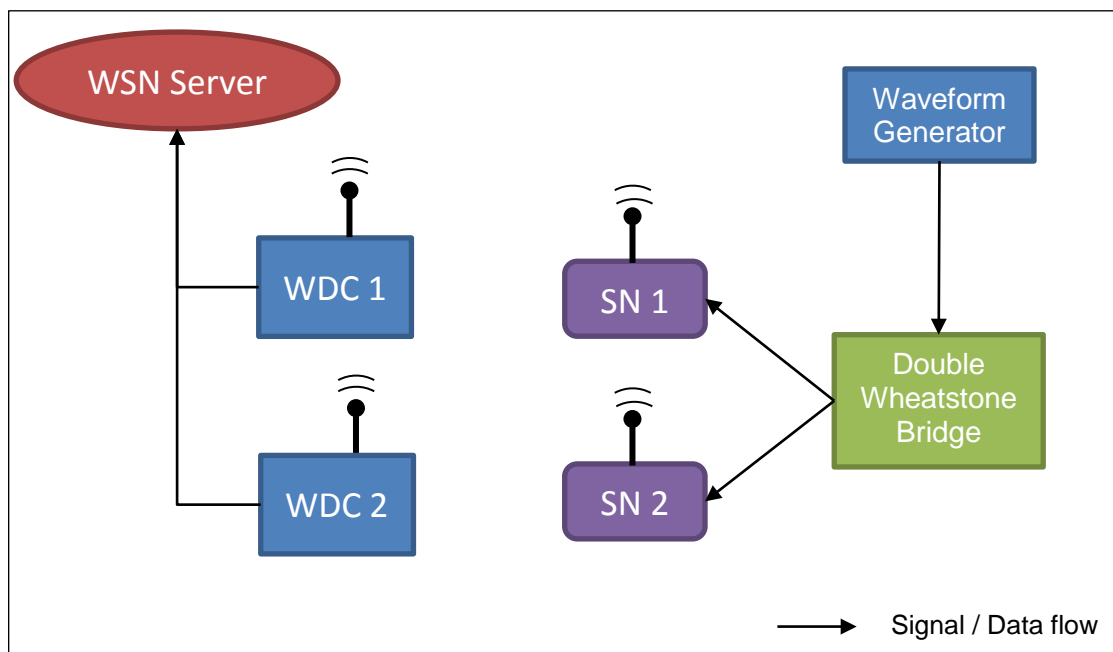


Figure 14: test setup with embedded devices. Two cells.

Data samples are collected by the WSN server and exported into Octave. The acquisition rate is 100 Hz. Measurement sessions lasted between 30 and 60 min. Figure 15 shows a portion of the data received by the server. This extract shows that the data acquisition works correctly as both data sets form a 1 Hz triangle of similar amplitude. The Y-axis offset between them is due to the uncertainty on the resistor values of the double Wheatstone bridge circuit used to acquire the same signal on two sensor nodes.

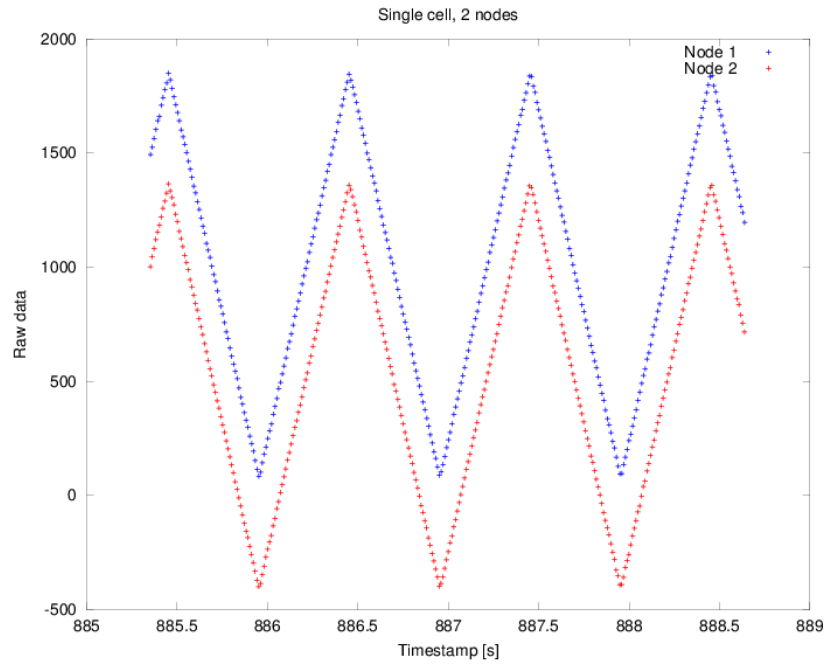


Figure 15: extract of the same triangle signal acquisition by two sensor nodes in one cell

The method to estimate the synchronisation error consists in measuring the time difference between the peaks of the triangle signal acquired by the two sensor nodes (Figure 16). For each phase of the triangle, the time of both acquired waveform peaks is computed using interpolation and intersection as explained in Figure 17.

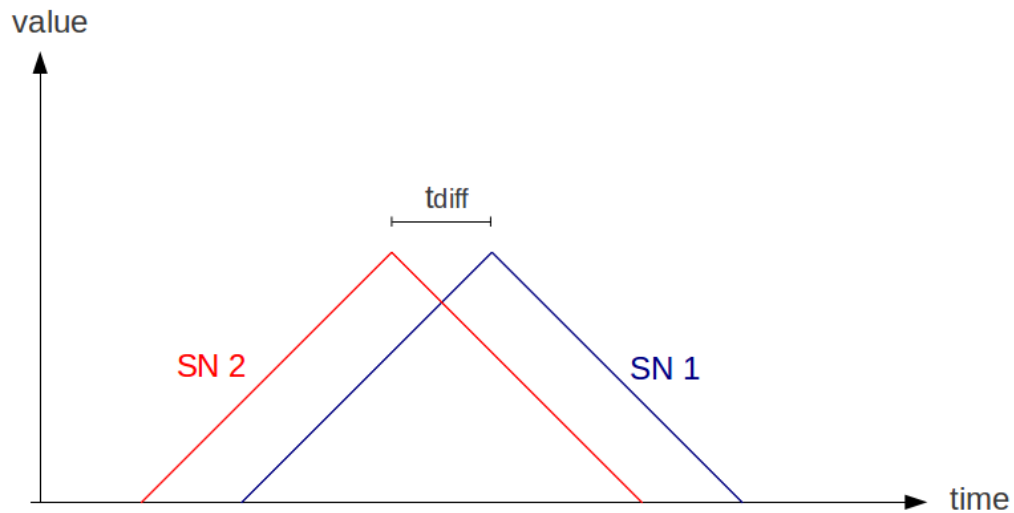


Figure 16: the synchronisation error is computed from the time difference between the two peaks of the acquisitions of the same triangle signal by sensor nodes 1 and 2

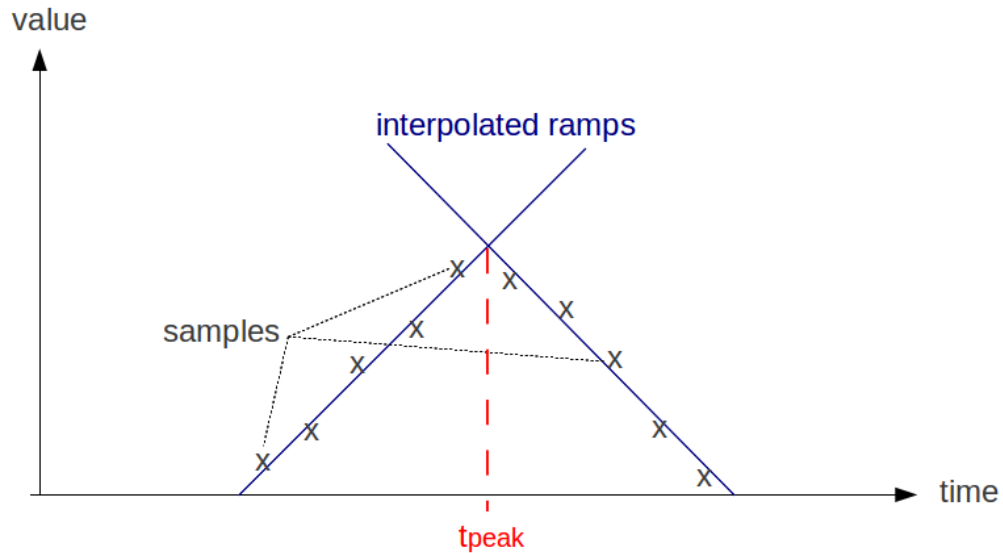


Figure 17: computation of peak time from data samples through interpolation and intersection

In the single cell configuration, only wireless synchronisation is active. Figure 18 shows the values obtained during an acquisition process of about an hour. The average error is 138 μ s whilst the maximal encountered error is 586 μ s.

In the two cells case, both wireless (WDC – SN) and wired (WSN server – WDC) synchronisation protocols are active. As expected, higher errors are observed as displayed in Figure 19. The average synchronisation error is 237 μ s and the maximal 878 μ s. This is a remarkable performance as the measured error lies well below the 1 ms specified by the user. In the two cells case, the two WDCs (Figure 14) are connected to the WSN server through a private network which is exclusive to the WDCs and the server. Hence higher errors should be expected in wider networks with switches and/or routers that would add extra random delays.

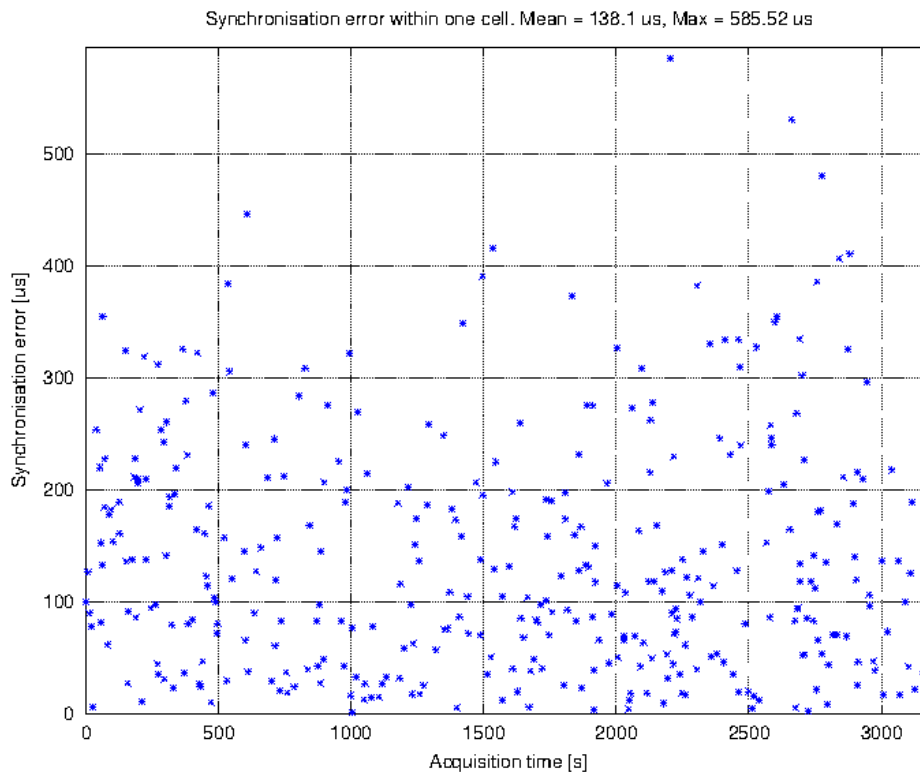


Figure 18: synchronisation error within one cell of two sensor nodes. Each point represents the synchronisation error computed on one cycle of the triangle waveform acquired by the sensor nodes.

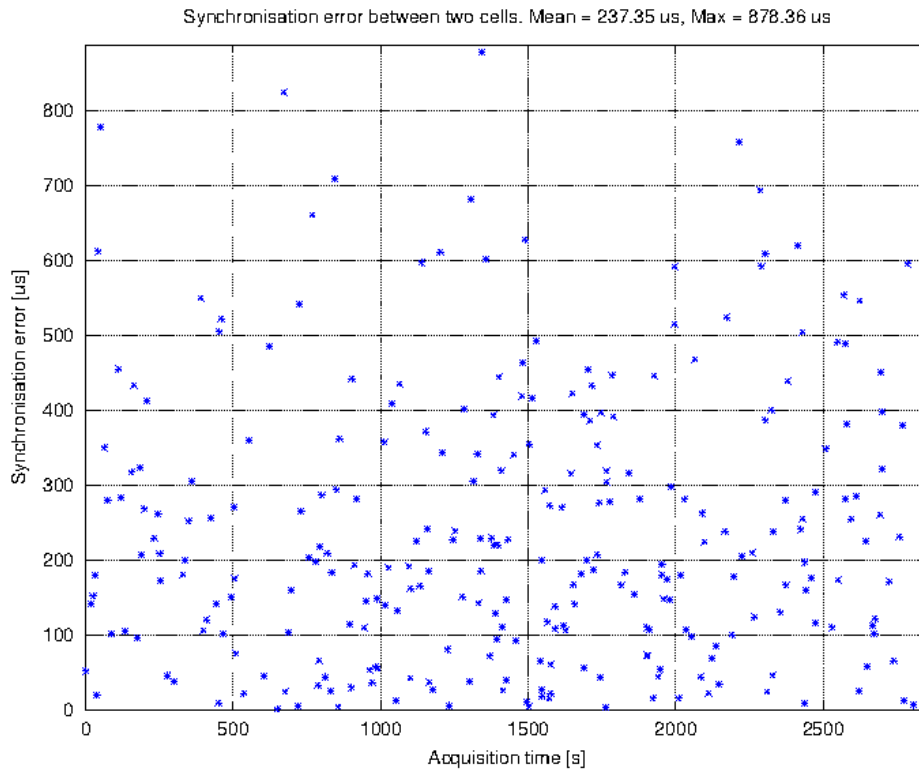


Figure 19: synchronisation error within two cells of one sensor node each. Each point represents the synchronisation error computed on one cycle of the triangle waveform acquired by the sensor nodes.

Both Figures above give a conservative estimate of the error. This is due to the measurement method which may increase the real synchronisation error: because the double Wheatstone circuit has been arranged with mainstream components (resistors, connectors), the input signals may be distorted. This could lead to errors in the voltage acquisition, resulting in an erroneous slope computation during the interpolation (Figure 17). In turn, this incurs a deviation in the triangle peak time estimate. As explained above, some detection algorithm has been used to rule out most of the erroneous acquisition. However, it is very likely that some errors have gone through the filter undetected.

Clock deviation is not the only source of synchronisation error, as correct synchronisation heavily depends on correct timestamp acquisition. To achieve this, it is necessary to acquire timestamp exactly when the wired or wireless network interface of the device sends or receive the packet, but implementation constraints (interrupt handling, avoiding software coupling) often result in unpredictable delays between actual packet emission or reception and timestamp recording. If the device is a mainstream personal computer, the operating system restricts the access to network interface low-level functions, thus obtaining accurate timestamp is even harder. In the future, it would be advisable to stick to standard synchronisation protocols for the wired network to allow benefiting from commercial synchronisation software and drivers. Another source of error is timer reading during timestamp acquisition. On the Texas Instruments MSP430 which equips the SN and WDC, this operation involves reading a running counter which may give erroneous results as detected by experiment.

Server to WDC synchronisation has been evaluated indirectly using data acquisition and the double Wheatstone bridge described above because a direct method would involve the precise simultaneous triggering of timestamp acquisition on the WSN server and one or more WDC. This could not be achieved within the frame of this work because the commercial computer used as a server did not provide access to some output signal without operating system random delays.

3.3 Power supply

3.3.1 Device Concept

The operating principle of heat storage thermoelectric harvesting can be described with reference to the device described in this report, which is illustrated in Figure 20. The heat storage unit (HSU) comprises a phase change material (PCM) inside a container which provides thermal contact to one or more thermoelectric generators (TEGs) and is otherwise thermally insulated from the environment. The PCM-TEG thermal properties are enhanced by a bridge structure which improves the temperature uniformity within the PCM. An insulation layer prevents heat leakage to the environment through the rest of the HSU surface. The outside TEG surface is in thermal contact with the environment. When the environmental temperature fluctuates, heat flows in and out of the HSU through the TEGs, resulting in generation of electrical energy. The energy output of the harvesting device can be collected, stored and distributed by a power management system.

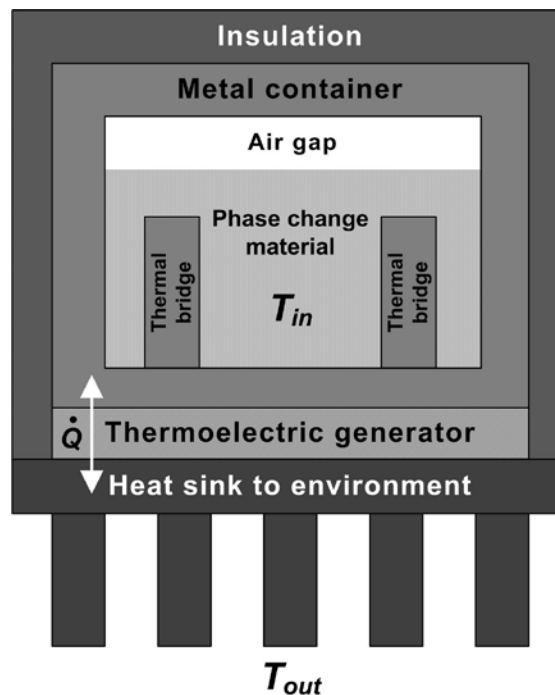


Figure 20: Schematic of the heat storage thermoelectric energy harvester.

In comparison with conventional thermoelectric harvesters, the objective function for optimization has a critical difference. In cases where a TEG is used to exploit a local temperature difference directly, the energy source can typically be approximated as a limitless supply of heat at constant temperature, with the input temperature to the TEG affected only by the finite thermal conductance of the source structure, not by the loss of energy through the TEG. Consequently, maximisation of energy output requires maximisation of the product of heat flow and TEG efficiency. Taking into account the approximately linear variation of η_{TEG} with ΔT , simple calculations show that the TEG thermal resistance should match that of the rest of the series thermal path between the high temperature source and the ambient. Thus optimum operation in direct thermoelectric harvesters occurs when the temperature difference across the TEG is $\Delta T/2$, in analogy with load matching in electrical power transfer. This thermal resistance matching requirement is illustrated in Figure 21a.

On the contrary, in heat storage thermoelectric harvesting the total available heat energy is limited, and hence maximization of conversion efficiency, rather than output power, is required. Consequently, a TEG with as large a thermal resistance as possible is desirable. An electrical analogy of this effect can be found in the discharge of a capacitor into a resistive load, through its own series resistance. As opposed to the case of power transfer from a voltage source where resistance matching is required, in the case of a capacitor discharge, maximization of the load resistance is required. This is shown in Figure 21b.

3.3.3 Power Electronics Interface

A power management system was developed in order to convert the generated voltage of the TEGs into a regulated output voltage and to store excess energy into a battery.

From the voltage profile shown in **Error! Reference source not found.**, it can be seen that a bipolar voltage is generated because ΔT changes sign midway through the complete cycle. Therefore it is necessary to incorporate a rectification stage into the power management system. However, due to the low voltages generated by the TEGs, simple bridge rectifiers are not suitable due to the diode voltage drops being comparable to the generated voltage of ± 0.8 V. In addition, it is desirable for the rectifier to cold-start, which precludes the use of conventional active rectification requiring gate drivers. A new rectifier topology was developed using a combination of off-the-shelf enhancement- and depletion-mode MOSFETs. These were configured such that the required rectification path is available at the beginning of the temperature cycle without gate drivers. A block diagram of the power management system is shown in Figure 23.

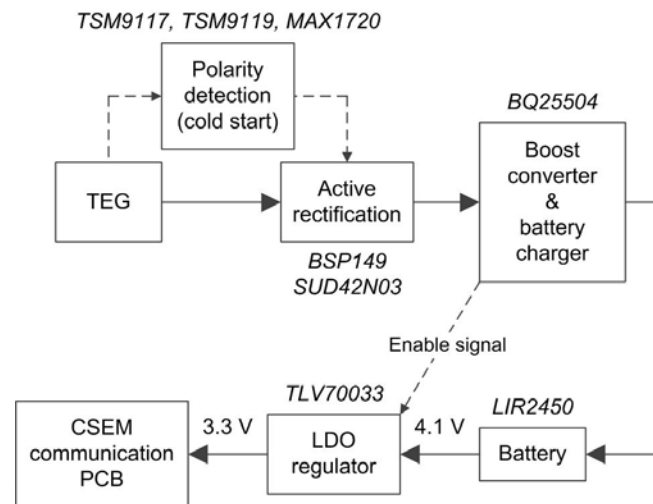


Figure 23: Block diagram of the power management electronics.

The complete power electronics interface consists of:

Two low-power comparators from Touchstone Semiconductor: TSM9117, TSM9119

Voltage inverter from Maxim: MAX1720

N-channel depletion and enhancement-mode MOSFETs: BSP149 and SUD42N03 respectively

Texas Instruments impedance-matching boost converter and battery charger: BQ25504

Rechargeable Lithium Ion battery 4.1 V, 120 mAh: LIR2450

A 3.3 V LDO regulator from Texas Instruments: TLV70033.

3.3.4 Power Supply Performance

The power supply performance has been characterised under laboratory-emulated flight temperature conditions. The generator harvests over 120 J from typical fuselage temperature profiles ranging from +20 °C to -25 °C and back. The TEG-to-battery efficiency of the power management system is 64%. This is the overall average efficiency for a complete flight cycle. The energy delivered into the battery was over 80 J. The device response to a typical flight scenario, including HSU temperature, TEG voltage, power flow and energy delivery is shown in Figure 24. The demonstrated laboratory performance shows that the delivered devices satisfy the size, energy and power requirements of the sensor node system.

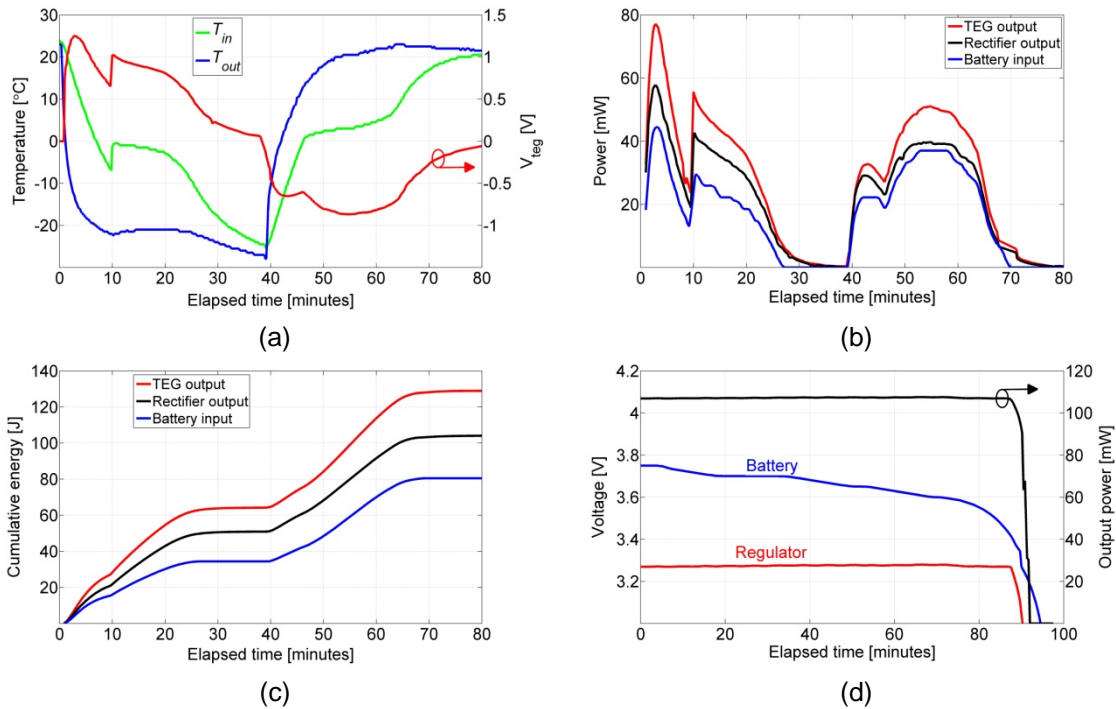


Figure 24: Performance of the StrainWiSe power supply: (a) HSU temperature and TEG voltage; (b) TEG and rectifier power output and power delivery to the battery; (c) Cumulative energy at the TEG output, rectifier output and battery input; (d) Power supply output voltage characterisation showing battery voltage, regulator voltage and output power on a 100Ω load.

3.4 Packaging

The StrainWiSe equipment must withstand high temperature differences and be resistant to humidity and vibrations.

Project partner Serma designed housings which are compliant with such requirements. Moreover, an important effort was dedicated to reduce and optimize the volume of the Sensor Node, and to provide a surface for securely installing it on the aircraft's structure (Figure 25).

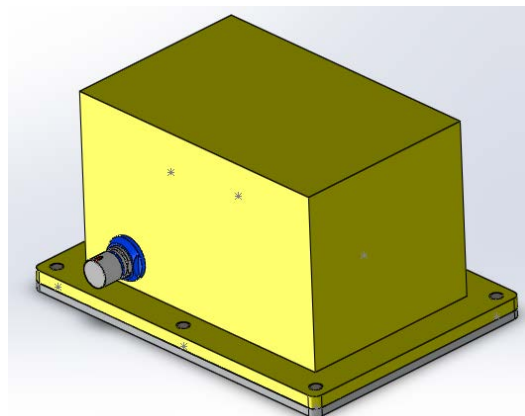


Figure 25: external aspect of the sensor node packaging

The body is in plastic and the base plate uses aluminium for the thermal conduction needs of the energy harvester. A four pins connector for the strain gauge sensor is placed on the bottom of the box and is directly soldered to the nearest PCB so that no cabling is necessary.

The sensor node comprises two electronics board and the heat storage unit of the thermo-electric energy harvester. The setup designed by Serma minimises volumes and connectors. It is displayed in Figure 26.

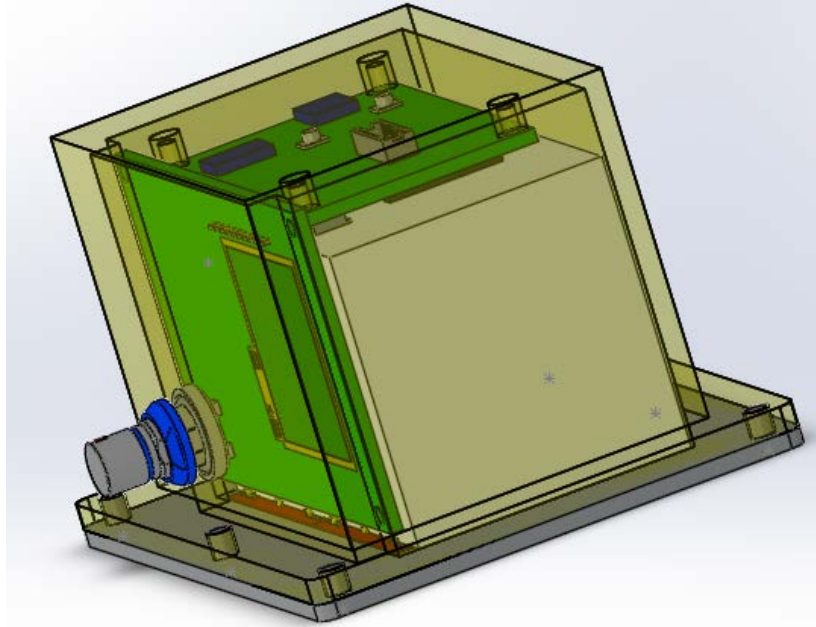


Figure 26: inside of the sensor node packaging. The power control PCB (Imperial College) is on the left of the heat storage unit and the data acquisition and communication PCB (CSEM) is on the top.

The two electronics boards are interconnected by a 10 pin connector as shown by Figure 27

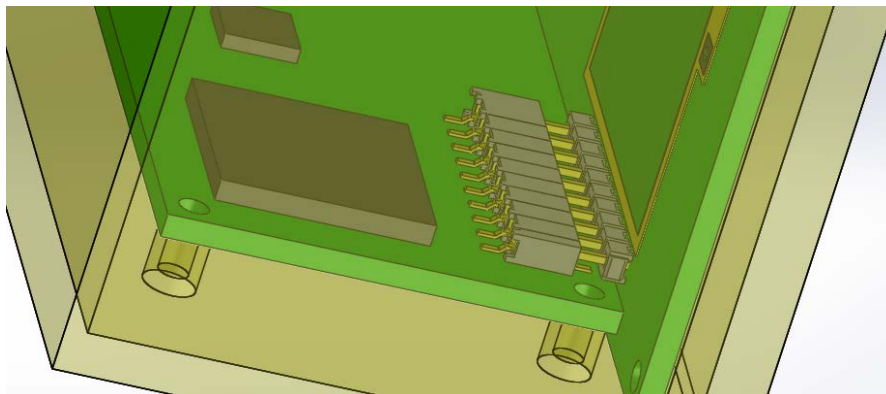


Figure 27: connector between the two electronic boards

As standard connectors could not be used because of the harvester design, it was decided to use spring contacts to connect the power electronics board with the output voltage of the thermo-electric generators placed beneath the heat storage unit (Figure 28).

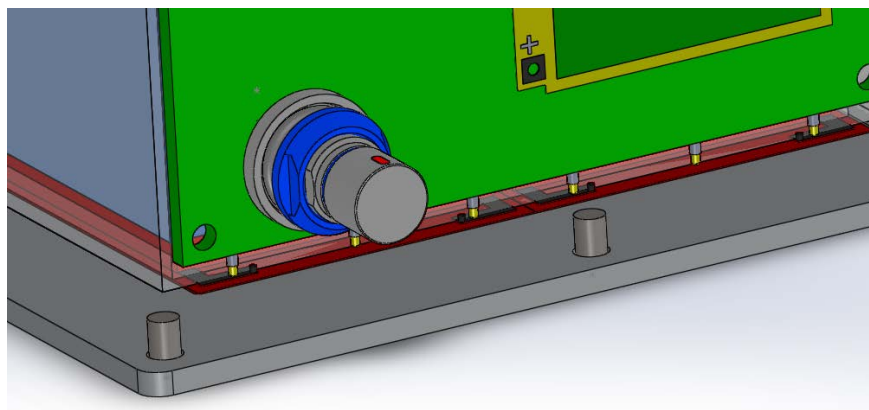


Figure 28: spring contacts used for connecting the energy harvester to the power PCB

A battery pack was developed to allow replacing the harvester power supply by a more conventional source when only the data acquisition and communication functionalities are tested. The Battery pack is made of 8 cells 3v3 lithium battery that will be located in a specifically designed plastic box occupying the volume dedicated to the harvester heat storage unit (*Figure 29*).

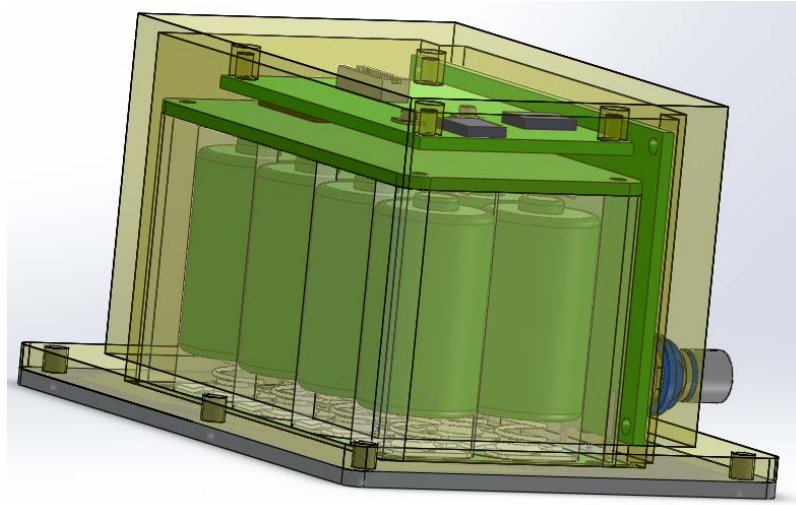


Figure 29: battery pack as an alternative power supply for the sensor node

The next four Figures show pictures of the manufactured housings.

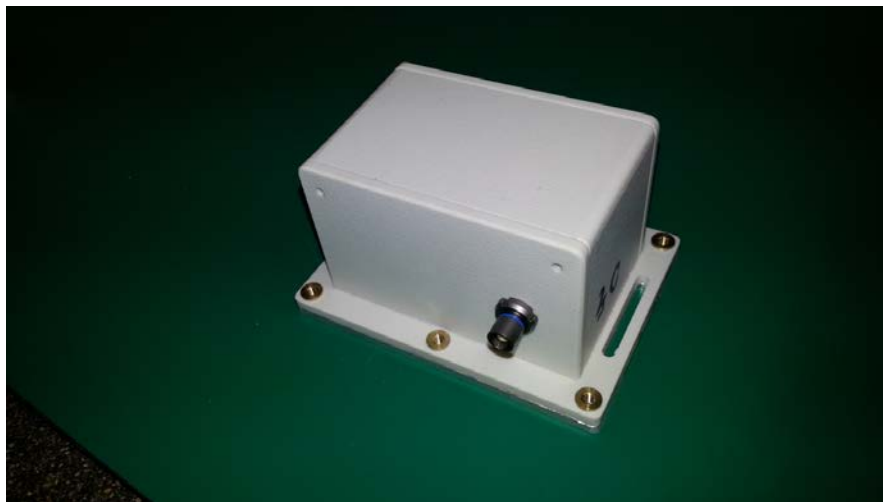


Figure 30: Integrated Sensor Node



Figure 31: Integrated WDC



Figure 32: Specific power supply electronic board for WDC

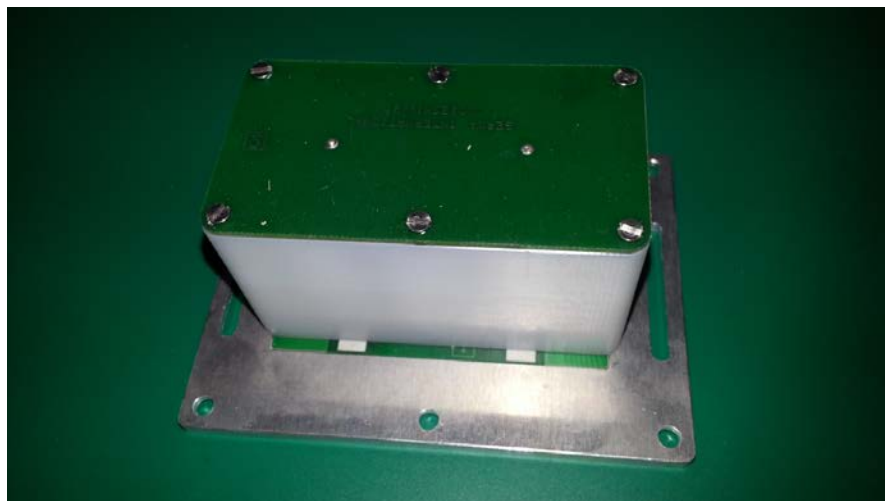


Figure 33: Battery pack

3.5 Functional and qualification tests

Testing the StrainWise system had two aspects: to ensure that it delivers the required functionality and to assess that it does not disturb the aircraft systems when used as an on-board demonstrator. The latter is required to obtain flight clearance from the Airbus flight test department.

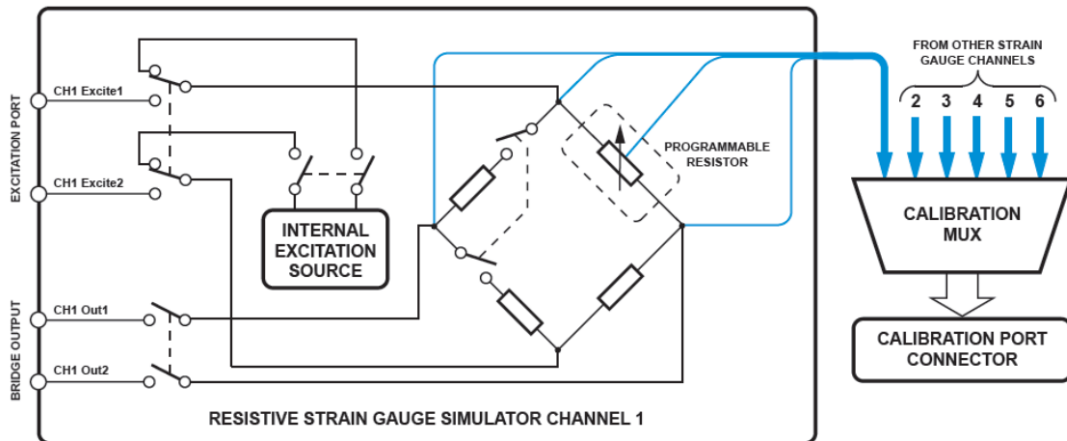
3.5.1 Functional tests

The main objectives of the functional tests are to determine the system correct functionality; to measure the sensor front-end accuracy; to evaluate the energy harvester performance and to assess the wireless communications.

3.5.1.1 Test setups

Typical test setups include the use of one WSN server, one or two WDC and one or several sensor nodes. Depending on the test, the sensor node is powered by battery pack or energy harvester. In the latter case, a climatic chamber is used to mimic a flight cycle temperature profile. Whenever strain measurements are part of a test, the sensor front-end is connected to a strain gauge simulator (Figure 34).

Figure 35 and Figure 36 depict typical test setups.



Functional Diagram for a single channel of the 40-265 Strain Gauge Simulator Module

Figure 34: Strain Gauge simulator (PXI Card)

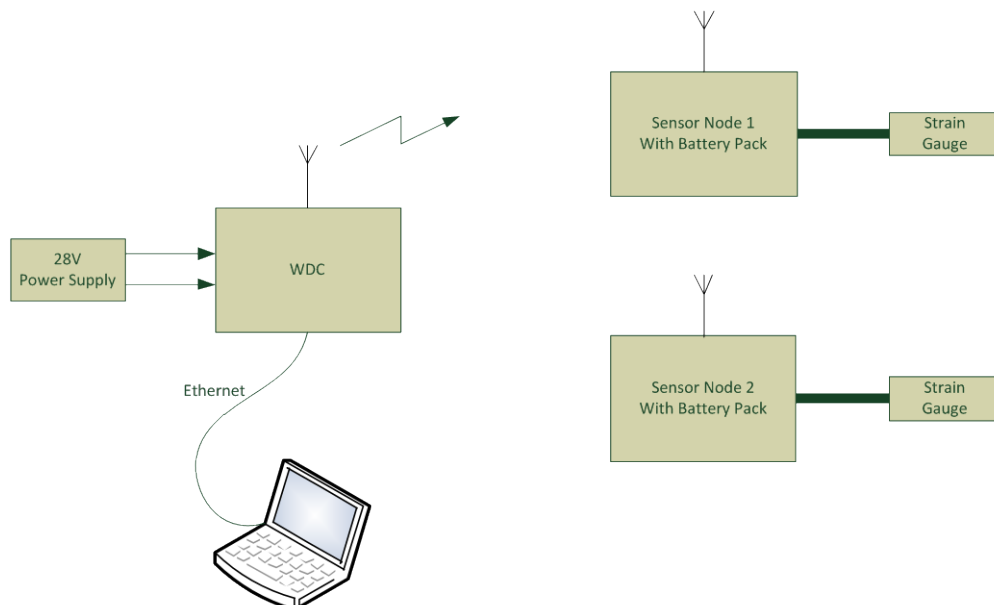


Figure 35: test setup with battery powered sensor nodes

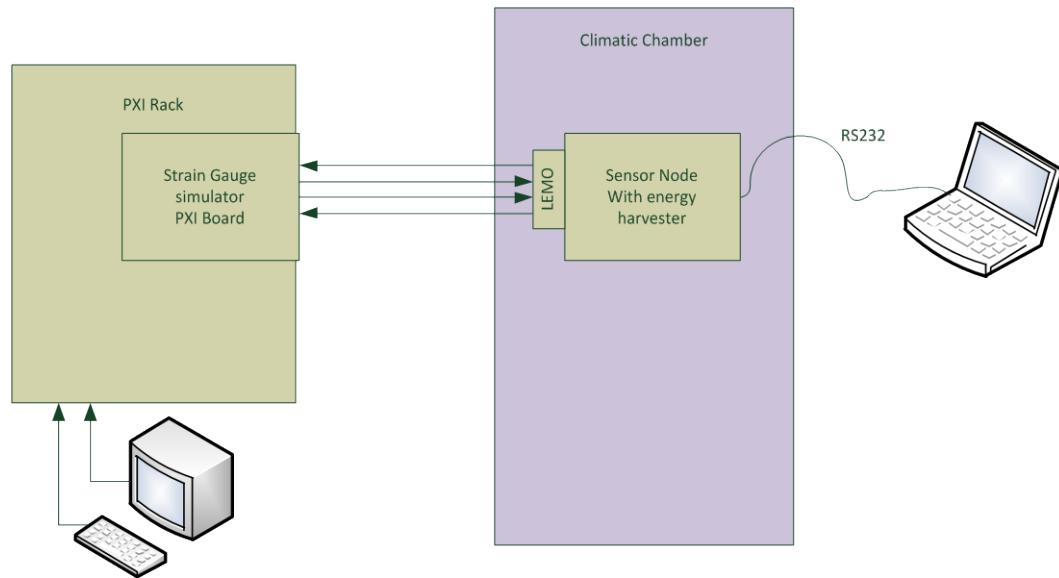


Figure 36: test setup with harvester-powered sensor node and strain gauge simulator

3.5.1.2 Test results

Functional test results are summarised in Table 1. The results code are:

- OK: test passed
- KO: test failed
- NT: Not Tested

Test	Result	Remark
Wake up method	OK	OK if MSP430 pins set to GPIOs when going to low power mode and reconfigured to original setting at wake-up. Not implemented.
Optimisation of low energy consumption	OK	
Keep alive signal	OK	
Communication with two WDCs	OK	
Identification number of Sensor Node	OK	
Net Id	OK	Net ID not necessary for the demonstrator, therefore the test passes.
Transmission Power	OK	
Communication with several Sensor Nodes	OK	
Antenna diversity	OK	
Communication with several WDC	OK	
Network capability	OK	
System monitoring	OK	All important commands are implemented and work properly. Some secondary commands are missing.
Measurement Time	KO	Feature not implemented in order to simplify the user interface as it is not necessary for the demonstrator. May be added as the Labview server is easily modifiable.
Measurement on request and periodic	KO	Measurements on request only. Periodic measurements session not necessary for a demonstrator. May be added as the Labview server is easily modifiable.
Measurement sample rate	OK	

Sample transmitting	OK	Delay between start and first data : mean = 335 ms, max = 534 ms
Simultaneous sensor node acquisition	OK	
AC time synchronisation	OK	Synchronisation with WSN server laptop time.
Temperature measurement	KO	Not implemented at time of testing. Implemented in prototypes delivered to the topic manager.
WSN data logging	OK	
Sensor node dimension	OK	Dimensions above Airbus specifications but accepted.
Sensor node mounting	OK	
ADC accuracy measurement	OK	
Strain gauge accuracy measurement	OK	
Strain gauge temperature accuracy measurement	OK	
Sensor Node and battery pack all range temperature validation	OK	
Test procedure with energy harvester configuration	OK	
Energy sufficiency and self-starting test	OK	

Table 1: summary of verification tests results

Most of the functionality tests of the Strainwise system pass, including the most important ones. Only minor deviations with respect to the specifications have been noticed. Thus the system is ready for flight tests as far as functionality was concerned.

3.5.2 Flight clearance

The Strainwise demonstrator is meant to be tested stand-alone without being connected to any system on board. Thus the flight clearance procedure is rather simple as the consortium has only to prove that the installation would not disturb any other equipment on board.

The flight clearance qualification test procedure is based on standard document DO160 "Environmental Conditions and Test Procedures for Airborne Equipment". The topic manager Airbus has cherry-picked the requirements that are necessary for the flight tests in this document. For the project, selected requirements are listed in Table 2.

Paragraph	Specification Requirement Paragraph	Description of Requirement (for information)	Category/method
Vibration : Group I	DO160 § 5.1	Vibrations (DO160F/ED14F, CHAP 8)	Category R Curve C1
Radiated Emission	DO 160 § 6.3	Emission of radio frequency energy (DO160F/ED14F, CHAP 21)	RE: CAT H

Table 2: flight clearance qualification requirements for the StrainWise system

These tests were performed at INTESPACES laboratory, Toulouse, France. Figure 37 and Figure 38 show the actual test setups.

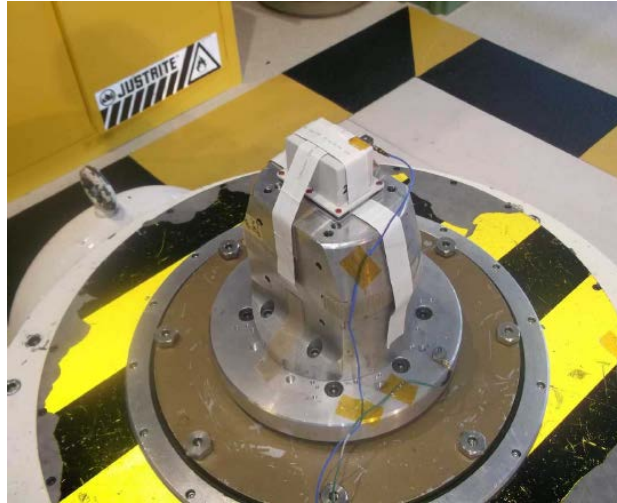


Figure 37: Sensor Node on vibration shaker on Z axis

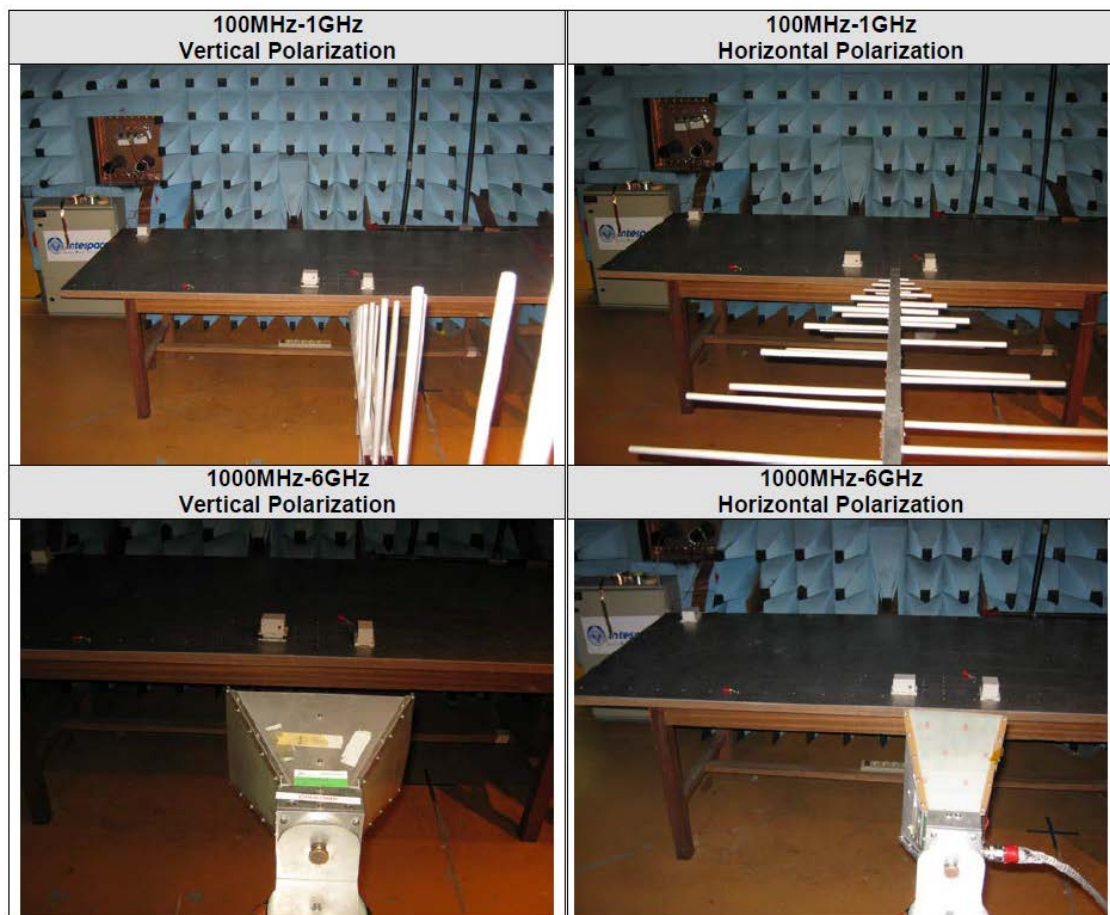


Figure 38: Two Sensor Nodes in radiated emission test

Only minor problems were detected during the qualification tests. The first problem was a leak in the seal of the energy scavenger heat storage unit. Improving the sealing fixed the issue. The second problem was a peak above limit detected during the radiated emissions test. It was caused by the Ethernet port of the WDC. Extra shielding was arranged to reduce the emission below the allowed limit.

4 Potential impact, dissemination and exploitation

(Please provide a description of the potential impact (including the socio-economic impact and the wider societal implications of the project so far) and the main dissemination activities and the exploitation of results. The length of this part cannot exceed 10 pages)

The present section discusses the project impact with respect to what was expected when writing the proposal. Then a summary of the dissemination activities follows. Finally, the section concludes with the presentation of the current and future exploitation plan.

4.1 Impact

The final outcome of the StrainWise project is the demonstrator of an energy-autonomous wireless airborne strain monitoring system. To the best of the consortium knowledge, this is the first fully integrated system that combines thermo-electrical energy harvesting and ultra-low power sensing, communication and synchronisation. Moreover, the demonstrator is qualified for flying as a flight test installation.

This represents a clear contribution to one of the Smart Fixed Wing Aircraft Integrated Technology Demonstrator (SFWA ITD) objectives, namely fuel burn reduction thanks to the reduced weight impact brought by replacing cables with lighter wireless sensor nodes.

Reducing fuel burn has a positive impact on the environment and increases the competitiveness of Europe's aviation industry because fuel consumption is a major criterion for the aircraft operators.

Other positive impacts resulting from the wireless nature of the StrainWise system are lower system operation costs due to reduced maintenance, reduced power requirements and management thanks to the use of energy harvesters, low risk of fire because some of the cabling and associated shielding is eliminated, and increased flexibility, for example, the ability to make changes. Finally, less cables also contributes to an easier aircraft architecture design.

Moreover, wireless solutions are obvious candidates for the retrofit of new features on existing aircrafts which may not provide room for extra wiring.

In longer terms, adding more and more sensors to aircrafts may result in even greater weight savings thanks to an increased knowledge which may lead to safely reducing the amount of material used to build the airframes.

The StrainWise system is a demonstrator and much effort will be needed to bring it into a product certified for commercial aircraft operation.

However, Flight Test Installations (FTI) are a potential short term customer for the system. Because they are not used in commercial operations, certification is easier. Also, such installations may require sensors in locations where cabling is very difficult if not impossible (for instance on propeller blades), thus wireless solutions are obvious candidates. Another benefit is cost reduction due to easier installation. Finally, the requirements on the energy harvesting are relaxed compared to full commercial operation. This simplifies the system device, thus speeds up the time to market.

4.2 Dissemination

Though not formally described in the description of work, the project conducted various dissemination activities. They are listed and classified below according to their nature.

4.2.1 Scientific papers

Published

M. E. Kiziroglou, S. W. Wright, T. T. Toh, P. D. Mitcheson and E. M. Yeatman, Heat Storage Harvesting on Aircrafts, Holistic ShowCase, 11.02.13, Imperial College London 2013.

M. E. Kiziroglou, S. W. Wright, T. T. Toh, T. Becker, P. D. Mitcheson and E. M. Yeatman, Heat Storage Power Supply For Wireless Aircraft Sensors, PowerMEMS 2012, Atlanta, Georgia, USA, Pages: 472-475 , December 02-05, 2012

E. M. Yeatman, Heat Storage Thermoelectric Energy Harvesting, NiPS 2012 Workshop on Energy harvesting: models and applications. Erice, Italy, July 23-27 2012.

M. E. Kiziroglou, D. Samson, T. Becker, S. W. Wright, and E. M. Yeatman, Optimization Of Heat Flow For Phase Change Thermoelectric Harvesters, PowerMEMS 2011, Seoul, Republic of Korea, Pages:454-457, November 15-18, 2011.

Accepted

Submitted

M. E. Kiziroglou, S. W. Wright, T. T. Toh, P. D. Mitcheson, T. Becker and E. M. Yeatman, Design and Fabrication of Heat Storage Thermoelectric Harvesting Devices, IEEE Trans. Industrial Electronics, under review, 2013.

Planned

T. T. Toh, S. W. Wright, M. E. Kiziroglou, E. M. Yeatman and P. D. Mitcheson, Phase Change Materials for Powering Aircraft Sensors, IEEE Transactions on Circuits and Systems II, to be submitted, 2013.

M. E. Kiziroglou, A. Elefsiniotis S. W. Wright, T. T. Toh, P. D. Mitcheson, T. Becker and E. M. Yeatman, Phase Change Materials for Powering Aircraft Sensors, App. Phys. Lett., to be submitted, 2013.

The consortium plans to write a paper on the overall project results once feed-back from flight tests will be received from Airbus. The target conference or journal hasn't been decided yet.

4.2.2 Within Cleansky SFWA ITD

The coordinator participated to several meetings of work package 1.3.6 of the Cleansky SFWA ITD:

- Meeting #9, Paris, June 21-22, 2011
- Meeting # 10, Madrid, October 27, 2011

4.2.3 Within the topic manager Airbus and EADS

The topic managers were issued from Airbus departments "Materials & Processes, NDT and Mechanical Testing" and Cabin Design Office Connectivity.

The project was widely disseminated within Airbus. The project deliverables have been made available on a dedicated section of Airbus internal portal "iShare".

In addition, specialists from other Airbus departments attended several project meetings. Their interests ranged from analytical structural health monitoring, to landing gear and flight test installation.

There has also been a fruitful collaboration between Imperial College and the EADS group active in energy scavenging during the course of the project. This collaboration resulted in joint publications including the PowerMEMS 2011 and PowerMEMS 2012 and two joint journal papers (one under review and one to be submitted).

4.2.4 To the general public

Project partner CSEM published two articles that promote the StrainWise in its annual scientific reports 2011⁵ and 2012⁶. The annual scientific reports are sent to a wide audience of CSEM stakeholders and published on CSEM website.

⁵ <http://www.csem.ch/docs/show.aspx/19790/docname/CSEM-STR-11.pdf>

⁶ Link not available yet

The StrainWise system was presented on TV on March 16, 2011 during an interview made by Swiss local TV BNJ TV on the aeronautical activities at CSEM⁷. BNJ TV is broadcasted on the Internet and covers the Swiss cantons of Neuchâtel, Jura and the French-spoken part of Bern (total inhabitants < 200'000).

4.3 Exploitation

The content of this section is confidential.

There are several on-going and future plans for the exploitation of the StrainWise results. They are presented below in chronological order.

4.3.1 Sensor nodes purchased by Airbus FTI

Airbus Flight Test Installation (FTI) department purchased two sensor nodes (with energy harvester) to test and demonstrate the benefits of energy-autonomous sensing internally. The nodes firmware was modified so that the acquired measurements were not transmitted but only saved on the internal flash memory instead.

4.3.2 New Cleansky project: Flite-Wise

The StrainWise consortium will continue working for Cleansky in a new project called "FLight Instrumentation TEst WIreless SEnsor – FLITE-WISE" in response to call for proposal JTI-CS-2012-03-SFWA-03-011.

The new project targets continuous measurements on rotating and non-rotating frames on the aircraft outer skin. It will start from the StrainWise platform and improve it towards higher acquisition rates (up to 50 kHz) and harsher environments (outside the aircraft, high centrifugal force). Size requirements will also be tighter (thickness) and alternative energy harvesting techniques will be studied.

The Flite-Wise project is promising for short term industrial exploitation because it targets flight-test installation, a market that is more mature than commercial aircraft systems for wireless applications.

4.3.3 Industrial partner Serma

Serma Ingénierie is the industrial partner of StrainWise. As such its plans for the exploitation of the project results are:

- Demonstrate to our main customers Eurocopter and Airbus Toulouse, that SERMA and its partners have acquired sufficient maturity to be able to propose industrial sensors, within wireless networks and low consumption.
- Furthermore, although Strainwise energy harvesting is not adapted to helicopter environment, this research development shows the capabilities to our team to manage efficiently this kind of problem.
- The promising result of this study, allow a good positioning of our consortium for as example on "Hélicoptère du Futur" new recherché program for Eurocopter.

Then at medium-term, SERMA intends to provide several type (temperature, strain gauge, pressure, acceleration, etc.) industrial autonomous sensors, allowing easily installation without bundle.

With this experience, we more easily find supplementary budgets, to pursue this research axis.

4.3.4 Imperial college

1. Cold starting Rectifier for heat-storage TEG harvesting (Commercial Exploitation of R&D results)

The novel rectifier topology developed for the StrainWiSe project addresses a problem that is common to energy harvesters with dual-polarity output. The followed approach can be interesting particularly for its integration into recently proposed power management microchips that have been implemented for multiple and heterogeneous energy harvesting sources. This would require co-designing particular implementations of the rectifier

⁷ <http://www.bnj.tv/fr/Video.html?idn=535&id=1353>

specifically with the maximum power point tracking system for an overall optimised system. The possibility of using depletion mode p-type MOSFETs at IC level should also be considered in order to further simplify and reduce the power consumption of the rectifier stage. Such a topology could not be exploited at PCB level due to the unavailability of p-channel depletion-mode MOSFETs as off-the-shelf components.

The proposed method of commercialisation consists of the presentation of the solution to relevant integrated circuit design companies and the negotiation of collaboration possibilities.

2. Power Supply for aircraft sensor nodes (Commercial Exploitation of R&D results)

The StrainWiSe power supply is based on a novel energy harvesting concept. The ability to harvest energy from aircraft temperature fluctuations and deliver it to a rechargeable battery is unique. The high energy output demonstrated for the generator (>126 J from a typical temperature flight cycle from +20 °C to -20 °C and back, with a total device volume of 78 cm³) and the demonstration of battery charging with overall efficiency of 64% leads to a remarkable total energy availability of 81 J per flight. The total volume of the unpackaged device including power management and energy storage electronics is 90 cm³. This amount of energy is more than three times the total energy consumption of the StrainWiSe sensor node during a full flight cycle.

The present implementation of the StrainWiSe power supply delivers enough energy for more demanding aircraft sensor applications. Nevertheless, there is considerable room for performance enhancement which may allow either for significant size reduction or energy increase. The main improvements that have been identified for the next iteration of the device are summarised in the following table.

Improvement Point	Required Effort (in PMs)	Estimated Energy Density Increase
Use of parallel depletion MOSFETs in rectifier	1	15%
Use of XPS (instead of PU)	1	5%
Minimisation of super-cooling and T-drift during phase change	>12	30%
Use of commercially available super-lattice TEGs (the estimate is for ZT = 0.8 at $\Delta T = 10$ °C)	6	>70%
Elimination of metal container (for smaller device sizes)	6	100%

Table 1: Identified improvement points for a power supply device upgrade.

3. Consortium know-how (General Advancement of Knowledge)

A major exploitable outcome of the StrainWiSe project is the consolidation of a highly complementary consortium among CSEM, Imperial and Serma. The experience gained through the development of the StrainWiSe sensor nodes provides a strong platform of cooperation, particularly on the parallel development of novel components towards products that meet particular specifications. The consortium envisions that the gained technological and coordination know-how will be exploited for the development of more energy-autonomous wireless sensor solutions in the future. In this respect the consortium has already been assigned a new JTI project in the same field, with the acronym FliteWiSe which is currently at the stage of negotiations.

4.3.5 CSEM

Partner CSEM will benefit from the results of StrainWISE through the application of its increased know-how and experience in the fields of low-power Wireless Sensor Networks (WSN), power management and sensor electronics. Low power WSN technology is needed to realize dependable, autonomous solutions for monitoring and surveillance capable of operation over extended periods and wide geographic areas. In accordance with CSEM's mission to bridge the gap between research and Industry, the technology developed in StrainWISE will be transferred into industrial developments. Potential applications for this technology extend beyond the domains of aeronautics to, for example, safety, health, automotive and transport applications.

Specifically, CSEM has added a new platform to its WSN solutions toolbox thanks to the StrainWise project. This new platform complements the existing Wisenet system which is based on the ultra-low power random access MAC WiseMAC as the TDMA nature of the new platform will allow CSEM to work where deterministic systems are mandatory.

The results of Strainwise will also be used in a currently running project for ESA in which a MAC protocol has to be proposed for UWB system using IEEE 802.15.4a physical layer for intra-satellite communications and wireless connections of ground test sensors.

5 Project public website

Not applicable.

However, the project material including reports, meeting minutes, PCB schematics and layout and user's guide had been uploaded into a section of Airbus supplier's portal dedicated to the project (access reserved to project's stakeholders):

<https://w4.airbus.com/sites/Structural/JTICS/default.aspx>